

$B \rightarrow X_s l^+ l^-$ in the left-right supersymmetric modelMariana Frank ¹ and Shuquan Nie ²

*Department of Physics, Concordia University, 1455 De Maisonneuve Blvd. W.
Montreal, Quebec, Canada, H3G 1M8*

We analyze the FCNC semileptonic decay $B \rightarrow X_s l^+ l^-$ in a fully left-right supersymmetric model. We give explicit expressions for all the amplitudes involved in the process, and compare the numerical results with experimental bounds, in both the constrained case (where the only flavor violation comes from the Cabibbo-Kobayashi-Maskawa matrix) and the unconstrained case (including soft breaking supersymmetry terms). Stringent constraints on the parameter space of the model are obtained. We also include constraints from $b \rightarrow s \gamma$.

PACS number(s): 12.60.Jv, 13.20.He, 13.20.-v

¹Email: mfrank@vax2.concordia.ca²Email: sxnie@alcor.concordia.ca

1 Introduction

Flavor changing neutral currents (FCNC) and charge parity (CP) violating phenomena are some of the best probes for physics beyond the Standard Model (SM). All existing measurements so far are consistent with the SM picture involving the Cabibbo-Kobayash-Maskawa (CKM) matrix as the only source of flavor violation. In the SM, FCNC are absent at tree level, appear at one loop, but they are effectively suppressed by the GIM mechanism and small CKM angles. In supersymmetry, there is no similar mechanism to suppress the loop contributions to either flavor or CP violating phenomena. Experimental studies of flavor physics, especially in B decays, appear essential for the understanding of the mechanism for supersymmetry breaking. With increased statistical power of experiments at B factories, rare B decays will be measured very precisely.

In this paper we investigate the relevance of new physics in the semileptonic inclusive decay $B \rightarrow X_s l^+ l^-$ in a fully left-right supersymmetric model. Investigation of the process $b \rightarrow s \gamma$ in this model has shown distinctive signs from the minimal supersymmetric standard model (MSSM) scenario [1]. An analysis of $B \rightarrow X_s l^+ l^-$ would provide some complementary information. The semileptonic decay $B \rightarrow X_s l^+ l^-$ is a benchmark of charmless b -decays with strange particles in the final state. The process is experimentally clean, but the expected SM branching ratio in the $10^{-6} - 10^{-5}$ region makes it not easily detectable at B-factories. Therefore it provides for excellent opportunities to test physics beyond the SM. It also offers more detailed information about the flavor structure of the model, it provides a good test of the structure of the Zbs vertex, making

it particularly well suited to distinguish the left-right symmetry over the MSSM.

Experimentally, BELLE has recently announced the first evidence for the exclusive process $B \rightarrow K^* l^+ l^-$. BABAR and BELLE have upper bounds for $B \rightarrow (K, K^*) + (e^+ e^-, \mu^+ \mu^-)$ which are very close to the SM estimates. Experimentally, the bounds on the branching ratios are [2]

$$\begin{aligned} BR(B \rightarrow X_s \mu^+ \mu^-) &< 19.1 \times 10^{-6} @ 90\% \text{ C.L.}, \\ BR(B \rightarrow X_s e^+ e^-) &< 10.1 \times 10^{-6} @ 90\% \text{ C.L.}, \end{aligned} \tag{1}$$

typically a factor of 3 away from the SM estimates, where the next-to-next-to leading logarithmic (NNLO) calculations to $\mathcal{O}(1/\alpha_s)$ [3] have appeared recently

$$\begin{aligned} BR(B \rightarrow X_s \mu^+ \mu^-) &< (4.15 \pm 0.70) \times 10^{-6}, \\ BR(B \rightarrow X_s e^+ e^-) &< (6.89 \pm 1.01) \times 10^{-6}. \end{aligned} \tag{2}$$

Here we restrict ourselves to the analysis of inclusive processes only: in the case of exclusive decay rates, hadronic matrix element uncertainties obscure model predictions.

Semileptonic charmless B decays have been studied previously by many authors in the framework of supersymmetric models with a universal soft supersymmetry breaking terms [4]. Recently an analysis of SUSY models with non-universal soft breaking terms at the grand unification scale has appeared in Ref. [5]. Although attempts have been made to reconcile $b \rightarrow s \gamma$ with right-handed b -quark decays [6], a complete analysis of $B \rightarrow X_s l^+ l^-$ for a fully left-right supersymmetric model is still lacking.

The Left-Right Supersymmetric (LRSUSY) models [7, 8], based on the symmetry group $SU(2)_L \times SU(2)_R \times U(1)_{B-L}$, incorporate the advantages

of supersymmetry with a natural framework for allowing neutrino masses through the seesaw mechanism [9]. Various other scenarios incorporate some forms of the left-right symmetry within supersymmetry. LRSUSY models have the attractive feature that they can be embedded in a supersymmetric grand unified theory such as $SO(10)$ [10], while not bound by lepton quark unification. They would also appear in model building realistic brane worlds from Type I strings. This involves the left-right supersymmetry, with supersymmetry broken either at the string scale $M_{SUSY} \approx 10^{10-12}$ GeV, or at $M_{SUSY} \approx 1$ TeV, the difference having implications for the gauge unification [11].

In this paper we study all contributions of the LRSUSY model to the branching ratio and the asymmetry of $B \rightarrow X_s l^+ l^-$ at one-loop level. The decay can be mediated by the left-handed and right-handed W and Z bosons, and by charged Higgs bosons as in the nonsupersymmetric case, but also by charginos, neutralinos and gluinos. The structure of the LRSUSY model provides a significant contributions to the decay $B \rightarrow X_s l^+ l^-$ from the right-handed squarks and an enlarged gaugino-Higgsino sector with right-handed couplings, which is not as constrained as the right-handed gauge sector in the LRSUSY model. We anticipate that these could contribute a large enhancement of the decay rate and would constrain some of the parameters of the model.

The paper is organized as follows. We describe the structure of the model in Sec. II, with particular emphasis on the gaugino-Higgsino and squark structure. In Sec. III, we give the supersymmetric contributions in the LRSUSY model to the decay $B \rightarrow X_s l^+ l^-$. We confront the calculation with experimental results in Sec. IV, where we present the numerical

analysis to constrain the parameters of the model for two scenarios: one with the CKM flavor mixing only, the other including supersymmetric soft breaking flavor violation terms. We reach our conclusions in Sec. V.

2 The Model

The LRSUSY electroweak symmetry group, $SU(2)_L \times SU(2)_R \times U(1)_{B-L}$, has matter doublets for both left- and right-handed fermions and their corresponding left- and right-handed scalar partners (sleptons and squarks) [8]. In the gauge sector, corresponding to $SU(2)_L$ and $SU(2)_R$, there are triplet gauge bosons $(W^+, W^-, W^0)_L$, $(W^+, W^-, W^0)_R$, respectively, and a singlet gauge boson V corresponding to $U(1)_{B-L}$, together with their superpartners. The Higgs sector of this model consists of two Higgs bidoublets, $\Phi_u(\frac{1}{2}, \frac{1}{2}, 0)$ and $\Phi_d(\frac{1}{2}, \frac{1}{2}, 0)$, which are required to give masses to the up and down quarks. The spontaneous symmetry breaking of the group $SU(2)_R \times U(1)_{B-L}$ to the hypercharge symmetry group $U(1)_Y$ is accomplished by giving vacuum expectation values to a pair of Higgs triplet fields $\Delta_L(1, 0, 2)$ and $\Delta_R(0, 1, 2)$, which transform as the adjoint representation of $SU(2)_R$. The choice of two triplets (versus four doublets) is preferred because with this choice a large Majorana mass can be generated (through the see-saw mechanism) for the right-handed neutrino and a small one for the left-handed neutrino [9]. In addition to the triplets $\Delta_{L,R}$, the model must contain two additional triplets, $\delta_L(1, 0, -2)$ and $\delta_R(0, 1, -2)$, with quantum number $B - L = -2$, to insure cancellation of the anomalies which would otherwise occur in the fermionic sector. The superpotential for the

LRSUSY model is

$$\begin{aligned}
W_{LRSUSY} = & \mathbf{h}_q^{(i)} Q^T \tau_2 \Phi_i \tau_2 Q^c + \mathbf{h}_l^{(i)} L^T \tau_2 \Phi_i \tau_2 L^c + i(\mathbf{h}_{LR} L^T \tau_2 \Delta_L L \\
& + \mathbf{h}_{LR} L^{cT} \tau_2 \Delta_R L^c) + M_{LR} [Tr(\Delta_L \delta_L + \Delta_R \delta_R)] \\
& + \mu_{ij} Tr(\tau_2 \Phi_i^T \tau_2 \Phi_j) + W_{NR},
\end{aligned} \tag{3}$$

where W_{NR} denotes (possible) non-renormalizable terms arising from higher scale physics or Planck scale effects [12]. The presence of these terms insures that, when the SUSY breaking scale is above M_{W_R} , the ground state is R-parity conserving [13].

The neutral Higgs fields acquire non-zero vacuum expectation values (VEV 's) through spontaneous symmetry breaking

$$\langle \Delta \rangle_{L,R} = \begin{pmatrix} 0 & 0 \\ v_{L,R} & 0 \end{pmatrix}, \text{ and } \langle \Phi \rangle_{u,d} = \begin{pmatrix} \kappa_{u,d} & 0 \\ 0 & \kappa'_{u,d} e^{i\omega} \end{pmatrix}.$$

$\langle \Phi \rangle_{u,d}$ cause the mixing of W_L and W_R bosons with CP -violating phase ω , which is set to zero in the analysis. The non-zero Higgs VEV 's break both parity and $SU(2)_R$. In the first stage of breaking, the right-handed gauge bosons, W_R and Z_R acquire masses proportional to v_R and become much heavier than the SM (left-handed) gauge bosons W_L and Z_L , which pick up masses proportional to κ_u and κ_d at the second stage of breaking.

In the supersymmetric sector of the model there are six singly-charged charginos, corresponding to $\tilde{\lambda}_L$, $\tilde{\lambda}_R$, $\tilde{\phi}_u$, $\tilde{\phi}_d$, $\tilde{\Delta}_L^\pm$, and $\tilde{\Delta}_R^\pm$. The model also has eleven neutralinos, corresponding to $\tilde{\lambda}_Z$, $\tilde{\lambda}_{Z'}$, $\tilde{\lambda}_V$, $\tilde{\phi}_{u1}^0$, $\tilde{\phi}_{u2}^0$, $\tilde{\phi}_{d1}^0$, $\tilde{\phi}_{d2}^0$, $\tilde{\Delta}_L^0$, $\tilde{\Delta}_R^0$, $\tilde{\delta}_L^0$, and $\tilde{\delta}_R^0$. Although Δ_L is not necessary for symmetry breaking [14], and is introduced only for preserving the left-right symmetry, both $\Delta_L^{--}(\tilde{\Delta}_L^{--})$ and its right-handed counterparts $\Delta_R^{--}(\tilde{\Delta}_R^{--})$ play very important roles in lepton phenomenology of the LRSUSY model. The doubly

charged Higgs and Higgsinos do not affect quark phenomenology, but the neutral and singly charged components do, through mixings in the chargino and neutralino mass matrices. We include only the $\tilde{\Delta}_R$ contribution in the numerical analysis.

The supersymmetric sources of flavor violation in the LRSUSY model come from either the Yukawa potential or the trilinear scalar couplings. The interactions of fermions with scalar (Higgs) fields have the following form

$$\begin{aligned}\mathcal{L}_Y &= \mathbf{h}_u \overline{Q}_L \Phi_u Q_R + \mathbf{h}_d \overline{Q}_L \Phi_d Q_R + \mathbf{h}_\nu \overline{L}_L \Phi_u L_R + \mathbf{h}_e \overline{L}_L \Phi_d L_R + H.c., \\ \mathcal{L}_M &= i\mathbf{h}_{LR}(L_L^T C^{-1} \tau_2 \Delta_L L_L + L_R^T C^{-1} \tau_2 \Delta_R L_R) + H.c.,\end{aligned}\tag{4}$$

where \mathbf{h}_u , \mathbf{h}_d , \mathbf{h}_ν and \mathbf{h}_e are the Yukawa couplings for the up and down quarks and neutrino and electron, respectively, and \mathbf{h}_{LR} is the coupling for the triplet Higgs bosons. The left-right symmetry requires all \mathbf{h} -matrices to be Hermitean in the generation space and \mathbf{h}_{LR} matrix to be symmetric. In the universal case, there is no intergenerational mixings for squarks and the only source of flavor mixing comes from the CKM matrix. We will analyze this case first. Next we will look at the case in which intergenerational mixings in the squark sector are permitted and consider the effect of intergenerational mixings on the rate of the process $B \rightarrow X_s l^+ l^-$.

3 The analytic formulas

The effective Hamiltonian for the decay $B \rightarrow X_s l^+ l^-$ at the scale μ in the LRSUSY model is given by

$$\mathcal{H}_{eff} = -\frac{4G_F}{\sqrt{2}} K_{tb} K_{ts}^* \sum_i [C_i(\mu) Q_i(\mu) + \tilde{C}_i(\mu) \tilde{Q}_i(\mu)].\tag{5}$$

The operators relevant to the process $b \rightarrow sl^+l^-$ in the LRSUSY model are

$$\begin{aligned}
Q_7 &= m_b(q_\nu/q^2)(\bar{s}i\sigma_{\mu\nu}P_Rb)(\bar{l}\gamma_\mu l), \\
\tilde{Q}_7 &= m_b(q_\nu/q^2)(\bar{s}i\sigma_{\mu\nu}P_Lb)(\bar{l}\gamma_\mu l), \\
Q_9 &= (\bar{s}\gamma_\mu P_Lb)(\bar{l}\gamma_\mu l), \\
\tilde{Q}_9 &= (\bar{s}\gamma_\mu P_Rb)(\bar{l}\gamma_\mu l), \\
Q_{10} &= (\bar{s}\gamma_\mu P_Lb)(\bar{l}\gamma_\mu\gamma_5l), \\
\tilde{Q}_{10} &= (\bar{s}\gamma_\mu P_Rb)(\bar{l}\gamma_\mu\gamma_5l).
\end{aligned} \tag{6}$$

The Wilson coefficients C_i and \tilde{C}_i are initially evaluated at the electroweak or soft supersymmetry breaking scale, then evolved down to the scale μ . In the SM and constrained SUSY models, \tilde{Q}_i contributions are generally suppressed by $\mathcal{O}(m_s/m_b)$ compared with the contributions from Q_i . However this is not the case in generic SUSY models such as non-universal models. In Ref. [5] the operator \tilde{Q}_7 was included in the analysis. Due to the left-right symmetry, we are motivated to consider all contributions from both chirality operators.

The decay $b \rightarrow sl^+l^-$ can be mediated by either the photon or the Z_L , Z_R bosons, or it can proceed through the box diagrams. As in the MSSM, the Z_L boson contributions dominate where there is explicit $SU(2)_L$ symmetry breaking, and the Z_R boson contributions are important where there is explicit $SU(2)_R$ symmetry breaking, i.e., both cases in which left and right squarks occur in the same loop diagram. In these cases, the Z diagrams are enhanced by $m_{\tilde{q}}^2/M_Z^2$ with respect to the photon graphs. This could be an order of magnitude for the regular Z_L boson, but only of order 1 for the Z_R boson. We describe these contributions in detail below.

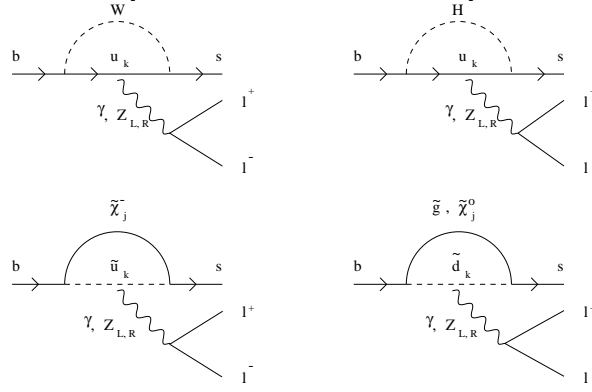


Figure 1: Penguin diagrams which induce the decay $b \rightarrow sl^+l^-$ in the LRSUSY model. The outgoing photon and Z boson lines can be attached in all possible ways.

3.1 The photon monopole and penguin graphs

The penguin monopole and dipole graphs are presented in Fig. 1. We first give the contributions for the constrained model, i.e., assuming the CKM matrix is the only source of flavor violation. The left-handed monopole contributions are given by

$$A_{SM}^{LL} = -\frac{\alpha_W \alpha}{2} \frac{1}{M_{W_L}^2} K_{ts}^* K_{tb} \{x_{tW} [Q_u F_7(x_{tW}) + F_8(x_{tW})] + \frac{2}{3} Q_u [\frac{\ln(x_{tW})}{x_{tW} - 1} - 1 + \ln(\frac{m_c^2}{M_{W_L}^2}) + f(\frac{q^2}{m_b^2})]\}, \quad (7)$$

$$A_{H^-}^{LL} = -\frac{\alpha_W \alpha}{2} \frac{1}{M_{W_L}^2} K_{ts}^* K_{tb} x_{tH} \cot^2 \beta [Q_u F_5(x_{tH}) - F_6(x_{tH})], \quad (8)$$

$$A_{\tilde{\chi}^-}^{LL} = -\alpha_W \alpha \sum_{j=1}^5 \sum_{k=1}^6 \frac{1}{m_{\tilde{u}_k}^2} (G_{UL}^{jkb} - H_{UR}^{jkb}) (G_{UL}^{*jks} - H_{UR}^{*jks}) \times [Q_u F_6(x_{\tilde{\chi}_j^- \tilde{u}_k}) - F_5(x_{\tilde{\chi}_j^- \tilde{u}_k})], \quad (9)$$

$$A_{\tilde{g}}^{LL} = -2\alpha_s \alpha C(R) Q_d \sum_{k=1}^6 \frac{1}{m_{\tilde{d}_k}^2} \Gamma_{DL}^{kb} \Gamma_{DL}^{*ks} F_6(x_{\tilde{g} \tilde{d}_k}), \quad (10)$$

$$A_{\tilde{\chi}^0}^{LL} = -\alpha_W \alpha Q_d \sum_{j=1}^9 \sum_{k=1}^6 \frac{1}{m_{\tilde{d}_k}^2} (\sqrt{2} G_{0DL}^{jkb} - H_{0DR}^{jkb}) (\sqrt{2} G_{0DL}^{*jks} - H_{0DR}^{*jks}) F_6(x_{\tilde{\chi}_j^0 \tilde{d}_k}). \quad (11)$$

The monopole contributions with W_L replaced by W_R , as in the left-right symmetric model (LRM), are suppressed by $\frac{M_{W_L}^2}{M_{W_R}^2}$ and thus negligible. The

only RR monopole contributions then come from the supersymmetric sector

$$A_{\tilde{\chi}^-}^{RR} = -\alpha_W \alpha \sum_{j=1}^5 \sum_{k=1}^6 \frac{1}{m_{\tilde{u}_k}^2} (G_{UR}^{jkb} - H_{UL}^{jkb}) (G_{UR}^{*jks} - H_{UL}^{*jks}) \times [Q_u F_6(x_{\tilde{\chi}_j^- \tilde{u}_k}) - F_5(x_{\tilde{\chi}_j^- \tilde{u}_k})], \quad (12)$$

$$A_{\tilde{g}}^{RR} = -2\alpha_s \alpha C(R) Q_d \sum_{k=1}^6 \frac{1}{m_{\tilde{d}_k}^2} \Gamma_{DR}^{kb} \Gamma_{DR}^{*ks} F_6(x_{\tilde{g} \tilde{d}_k}), \quad (13)$$

$$A_{\tilde{\chi}^0}^{RR} = -\alpha_W \alpha Q_d \sum_{j=1}^9 \sum_{k=1}^6 \frac{1}{m_{\tilde{d}_k}^2} (\sqrt{2} G_{0DR}^{jkb} - H_{0DL}^{jkb}) (\sqrt{2} G_{0DR}^{*jks} - H_{0DL}^{*jks}) F_6(x_{\tilde{\chi}_j^0 \tilde{d}_k}). \quad (14)$$

The dipole LR and RL contributions can be obtained by multiplying the contributions to the decay $b \rightarrow s\gamma$ by the factor $\sqrt{4\pi\alpha}$

$$A_{SM}^{LR} = \frac{\alpha\alpha_W}{2} \frac{1}{M_{W_L}^2} K_{ts}^* K_{tb} 3x_{tW} [Q_u F_1(x_{tW}) + F_2(x_{tW})], \quad (15)$$

$$A_{H^-}^{LR} = \frac{\alpha\alpha_W}{2} \frac{1}{M_{W_L}^2} K_{ts}^* K_{tb} x_{tH} \{ \cot^2 \beta [Q_u F_1(x_{tH}) + F_2(x_{tH})] + [Q_u F_3(x_{tH}) + F_4(x_{tH})] \}, \quad (16)$$

$$A_{\tilde{g}}^{LR} = -2\alpha\alpha_s Q_d C(R) \sum_{k=1}^6 \frac{1}{m_{\tilde{d}_k}^2} \{ \Gamma_{DL}^{kb} \Gamma_{DL}^{*ks} F_2(x_{\tilde{g} \tilde{d}_k}) - \frac{m_{\tilde{g}}}{m_b} \Gamma_{DR}^{kb} \Gamma_{DL}^{*ks} F_4(x_{\tilde{g} \tilde{d}_k}) \}, \quad (17)$$

$$A_{\tilde{\chi}^-}^{LR} = -\alpha\alpha_W \sum_{j=1}^5 \sum_{k=1}^6 \frac{1}{m_{\tilde{u}_k}^2} \{ (G_{UL}^{jkb} - H_{UR}^{jkb}) (G_{UL}^{*jks} - H_{UR}^{*jks}) [F_1(x_{\tilde{\chi}_j^- \tilde{u}_k}) + Q_u F_2(x_{\tilde{\chi}_j^- \tilde{u}_k})] + \frac{m_{\tilde{\chi}_j^-}}{m_b} (G_{UR}^{jkb} - H_{UL}^{jkb}) (G_{UL}^{*jks} - H_{UR}^{*jks}) [F_3(x_{\tilde{\chi}_j^- \tilde{u}_k}) + Q_u F_4(x_{\tilde{\chi}_j^- \tilde{u}_k})] \}, \quad (18)$$

$$A_{\tilde{\chi}^0}^{LR} = -\alpha\alpha_W Q_d \sum_{j=1}^9 \sum_{k=1}^6 \frac{1}{m_{\tilde{d}_k}^2} \{ (\sqrt{2} G_{0DL}^{jkb} - H_{0DR}^{jkb}) (\sqrt{2} G_{0DL}^{*jks} - H_{0DR}^{*jks}) F_2(x_{\tilde{\chi}_j^0 \tilde{d}_k}) + \frac{m_{\tilde{\chi}_j^0}}{m_b} (\sqrt{2} G_{0DR}^{jkb} - H_{0DL}^{jkb}) (\sqrt{2} G_{0DL}^{*jks} - H_{0DR}^{*jks}) F_4(x_{\tilde{\chi}_j^0 \tilde{d}_k}) \}, \quad (19)$$

and

$$A_{\tilde{g}}^{RL} = -2\alpha\alpha_s Q_d C(R) \sum_{k=1}^6 \frac{1}{m_{\tilde{d}_k}^2} \{ \Gamma_{DR}^{kb} \Gamma_{DR}^{*ks} F_2(x_{\tilde{g} \tilde{d}_k}) - \frac{m_{\tilde{g}}}{m_b} \Gamma_{DL}^{kb} \Gamma_{DR}^{*ks} F_4(x_{\tilde{g} \tilde{d}_k}) \}, \quad (20)$$

$$A_{\tilde{\chi}^-}^{RL} = -\alpha\alpha_W \sum_{j=1}^5 \sum_{k=1}^6 \frac{1}{m_{\tilde{u}_k}^2} \{ (G_{UR}^{jkb} - H_{UL}^{jkb}) (G_{UR}^{*jks} - H_{UL}^{*jks}) [F_1(x_{\tilde{\chi}_j^- \tilde{u}_k}) + Q_u F_2(x_{\tilde{\chi}_j^- \tilde{u}_k})] + \frac{m_{\tilde{\chi}_j^-}}{m_b} (G_{UL}^{jkb} - H_{UR}^{jkb}) (G_{UR}^{*jks} - H_{UL}^{*jks}) [F_3(x_{\tilde{\chi}_j^- \tilde{u}_k}) + Q_u F_4(x_{\tilde{\chi}_j^- \tilde{u}_k})] \}, \quad (21)$$

$$\begin{aligned}
A_{\tilde{\chi}^0}^{RL} &= -\alpha\alpha_W Q_d \sum_{j=1}^9 \sum_{k=1}^6 \frac{1}{m_{\tilde{d}_k}^2} \{ (\sqrt{2}G_{0DR}^{jkb} - H_{0DL}^{jkb})(\sqrt{2}G_{0DR}^{*jks} - H_{0DL}^{*jks}) F_2(x_{\tilde{\chi}_j^0 \tilde{d}_k}) \\
&\quad + \frac{m_{\tilde{\chi}_j^0}}{m_b} (\sqrt{2}G_{0DL}^{jkb} - H_{0DR}^{jkb})(\sqrt{2}G_{0DR}^{*jks} - H_{0DL}^{*jks}) F_4(x_{\tilde{\chi}_j^0 \tilde{d}_k}) \}, \tag{22}
\end{aligned}$$

where vertex mixing matrices G , H , G_0 and H_0 are defined in the Appendix.

The convention $x_{ab} = m_a^2/m_b^2$ is used. $C(R) = 4/3$ is the quadratic Casimir operator of the fundamental representation of $SU(3)_C$.

3.2 The Z_L , Z_R penguin graphs

The process $b \rightarrow sl^+l^-$ is also induced by the effective couplings of the Z_L and Z_R . The diagrams are analogous to the photon graphs where the photon is replaced by the Z propagator. The amplitudes for the Z_L mediated graphs are

$$A_{SM}^{Z_L} = -\frac{\alpha_W^2}{2} \frac{1}{M_{Z_L}^2 \cos^2 \theta_W} K_{ts}^* K_{tb} x_{tW} F_9(x_{tW}), \tag{23}$$

$$A_{H^-}^{Z_L} = -\frac{\alpha_W^2}{4} \frac{1}{M_{Z_L}^2 \cos^2 \theta_W} K_{ts}^* K_{tb} \cot^2 \beta x_{tW} x_{tH} [F_3(x_{tH}) + F_4(x_{tH})], \tag{24}$$

$$A_{\tilde{g}}^{Z_L} = -\alpha_W \alpha_s C(R) \frac{1}{M_{Z_L}^2 \cos^2 \theta_W} \sum_{h,k=1}^6 \Gamma_{DL}^{kb} \Gamma_{DL}^{*hs} \sum_{m=1}^3 \Gamma_{DR}^{hm} \Gamma_{DR}^{*km} G_0(x_{\tilde{d}_k \tilde{g}}, x_{\tilde{d}_h \tilde{g}}), \tag{25}$$

$$\begin{aligned}
A_{\tilde{\chi}^-}^{Z_L} &= -\frac{\alpha_W \alpha}{2} \frac{1}{M_{Z_L}^2 \cos^2 \theta_W} \sum_{h,k=1}^6 \sum_{i,j=1}^5 (G_{UL}^{jkb} - H_{UR}^{jkb})(G_{UL}^{*ihs} - H_{UR}^{*ihs}) \\
&\quad \times \left\{ \delta_{ij} \sum_{m=1}^3 \Gamma_{UL}^{hm} \Gamma_{UL}^{*km} G_0(x_{\tilde{u}_h \tilde{\chi}_i^-}, x_{\tilde{u}_k \tilde{\chi}_j^-}) + \delta_{hk} [2\sqrt{x_{\tilde{\chi}_j^- \tilde{u}_k} x_{\tilde{\chi}_i^- \tilde{u}_k}} F_0(x_{\tilde{\chi}_j^- \tilde{u}_k}, x_{\tilde{\chi}_i^- \tilde{u}_k}) \right. \\
&\quad \left. \times U_{i1} U_{j1}^* - G_0(x_{\tilde{\chi}_j^- \tilde{u}_k}, x_{\tilde{\chi}_i^- \tilde{u}_k}) V_{i1}^* V_{j1}] \right\}, \tag{26}
\end{aligned}$$

$$\begin{aligned}
A_{\tilde{\chi}^0}^{Z_L} &= -\frac{\alpha_W \alpha}{2} \frac{1}{M_{Z_L}^2 \cos^2 \theta_W} \sum_{h,k=1}^6 \sum_{i,j=1}^9 (\sqrt{2}G_{0DL}^{jkb} - H_{0DR}^{jkb})(\sqrt{2}G_{0DL}^{*ihs} - H_{0DR}^{*ihs}) \\
&\quad \times \left\{ \delta_{ij} \sum_{m=1}^3 \Gamma_{DL}^{hm} \Gamma_{DL}^{*km} G_0(x_{\tilde{d}_h \tilde{\chi}_i^0}, x_{\tilde{d}_k \tilde{\chi}_j^0}) + \delta_{hk} [2\sqrt{x_{\tilde{\chi}_j^0 \tilde{d}_k} x_{\tilde{\chi}_i^0 \tilde{d}_k}} F_0(x_{\tilde{\chi}_j^0 \tilde{d}_k}, x_{\tilde{\chi}_i^0 \tilde{d}_k}) \right. \\
&\quad \left. \times (N_{i4} N_{j4}^* - N_{i5} N_{j5}^*) - G_0(x_{\tilde{\chi}_j^0 \tilde{d}_k}, x_{\tilde{\chi}_i^0 \tilde{d}_k})(N_{i4}^* N_{j4} - N_{i5}^* N_{j5}) \right\}, \tag{27}
\end{aligned}$$

where we have included in the expressions both cases in which one vertex is gaugino and the other Higgsino, and the case in which we have two gaugino vertices. Similarly we obtain, for the Z_R mediated graphs

$$A_{\tilde{g}}^{Z_R} = -\alpha_W \alpha_s C(R) \frac{\cos 2\theta_W}{M_{Z_R}^2 \cos^2 \theta_W} \sum_{h,k=1}^6 \Gamma_{DR}^{kb} \Gamma_{DR}^{*hs} \sum_{m=1}^3 \Gamma_{DL}^{hm} \Gamma_{DL}^{*km} G_0(x_{\tilde{d}_k \tilde{g}}, x_{\tilde{d}_h \tilde{g}}), \quad (28)$$

$$\begin{aligned} A_{\tilde{\chi}^-}^{Z_R} &= -\frac{\alpha_W \alpha}{2} \frac{\cos 2\theta_W}{M_{Z_R}^2 \cos^2 \theta_W} \sum_{h,k=1}^6 \sum_{i,j=1}^5 (G_{UR}^{jkb} - H_{UL}^{jkb})(G_{UR}^{*ihs} - H_{UL}^{*ihs}) \\ &\times \left\{ \delta_{ij} \sum_{m=1}^3 \Gamma_{UR}^{hm} \Gamma_{UR}^{*km} G_0(x_{\tilde{u}_h \tilde{\chi}_i^-}, x_{\tilde{u}_k \tilde{\chi}_j^-}) + \delta_{hk} [2\sqrt{x_{\tilde{\chi}_j^- \tilde{u}_k} x_{\tilde{\chi}_i^- \tilde{u}_k}} F_0(x_{\tilde{\chi}_j^- \tilde{u}_k}, x_{\tilde{\chi}_i^- \tilde{u}_k}) \right. \\ &\times U_{i2} U_{j2}^* - G_0(x_{\tilde{\chi}_j^- \tilde{u}_k}, x_{\tilde{\chi}_i^- \tilde{u}_k}) V_{i2}^* V_{j2}] \left. \right\}, \quad (29) \end{aligned}$$

$$\begin{aligned} A_{\tilde{\chi}^0}^{Z_R} &= -\frac{\alpha_W \alpha}{2} \frac{\cos 2\theta_W}{M_{Z_R}^2 \cos^2 \theta_W} \sum_{h,k=1}^6 \sum_{i,j=1}^9 (\sqrt{2} G_{0DR}^{jkb} - H_{0DL}^{jkb})(\sqrt{2} G_{0DR}^{*ihs} - H_{0DL}^{*ihs}) \\ &\times \left\{ \delta_{ij} \sum_{m=1}^3 \Gamma_{DR}^{hm} \Gamma_{DR}^{*km} G_0(x_{\tilde{d}_h \tilde{\chi}_i^0}, x_{\tilde{d}_k \tilde{\chi}_j^0}) + \delta_{hk} [2\sqrt{x_{\tilde{\chi}_j^0 \tilde{d}_k} x_{\tilde{\chi}_i^0 \tilde{d}_k}} F_0(x_{\tilde{\chi}_j^0 \tilde{d}_k}, x_{\tilde{\chi}_i^0 \tilde{d}_k}) \right. \\ &\times (N_{i4} N_{j4}^* - N_{i5} N_{j5}^*) - G_0(x_{\tilde{\chi}_j^0 \tilde{d}_k}, x_{\tilde{\chi}_i^0 \tilde{d}_k})(N_{i4}^* N_{j4} - N_{i5}^* N_{j5}) \left. \right\}. \quad (30) \end{aligned}$$

As in the MSSM [4], when the $Z_{L,R}$ bosons are exchanged, gluino- and neutralino-induced contributions to the total amplitudes are suppressed by $\mathcal{O}(q^2/M_{Z_{L,R}}^2)$ with respect to the photon penguin contributions. In addition, the Z_R contribution is suppressed with respect to the left-handed one by $\mathcal{O}(M_{Z_L}^2/M_{Z_R}^2)$.

3.3 The box diagrams

The box graphs are presented in Fig. 2. The explicit contributions are given by

$$\begin{aligned} A_{SM}^{\square} &= -\frac{\alpha_W^2}{4} \frac{1}{M_{W_L}^2} K_{ts}^* K_{tb} [G(x_{tW}, 0) - G(0, 0)], \quad (31) \\ A_{\tilde{\chi}^-}^{L\square} &= \frac{\alpha_W^2}{4} \sum_{h,k=1}^6 \sum_{i,j=1}^5 \frac{1}{m_{\tilde{\chi}_i^-}^2} (G_{UL}^{jkb} - H_{UR}^{jkb})(G_{UL}^{*iks} - H_{UR}^{*iks}) \end{aligned}$$

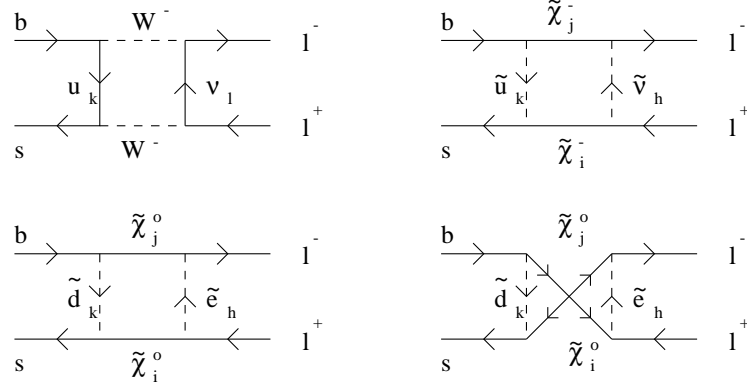


Figure 2: Box diagrams contributing to the decay $b \rightarrow sl^+l^-$ in the LRSUSY model. Clashing arrows on the fermion lines indicate a Majorana mass insertion.

$$\times G_{NL}^{*jhl} G_{NL}^{ihl} G'(x_{\tilde{u}_k \tilde{\chi}_j^-}, x_{\tilde{\nu}_h \tilde{\chi}_j^-}, x_{\tilde{\chi}_i^- \tilde{\chi}_j^-}), \quad (32)$$

$$A_{\tilde{\chi}^0}^{L\Box} = \frac{\alpha_W^2}{2} \sum_{h,k=1}^6 \sum_{i,j=1}^9 \frac{1}{m_{\tilde{\chi}_j^0}^2} (\sqrt{2} G_{0DL}^{jkb} - H_{0DR}^{jkb}) (\sqrt{2} G_{0DL}^{*iks} - H_{0DR}^{*iks}) \left[G_{0EL}^{*jhl} G_{0EL}^{ihl} \right. \\ \left. \times G'(x_{\tilde{d}_k \tilde{\chi}_j^0}, x_{\tilde{l}_h \tilde{\chi}_j^0}, x_{\tilde{\chi}_i^0 \tilde{\chi}_j^0}) - 2 G_{0EL}^{*ihl} G_{0EL}^{jhl} \sqrt{x_{\tilde{\chi}_i^0 \tilde{\chi}_j^0}} F'(x_{\tilde{d}_k \tilde{\chi}_j^0}, x_{\tilde{l}_h \tilde{\chi}_j^0}, x_{\tilde{\chi}_i^0 \tilde{\chi}_j^0}) \right], \quad (33)$$

$$A_{\tilde{\chi}^0}^{L\Box'} = -\frac{\alpha_W^2}{2} \sum_{h,k=1}^6 \sum_{i,j=1}^9 \frac{1}{m_{\tilde{\chi}_j^0}^2} (\sqrt{2} G_{0DL}^{jkb} - H_{0DR}^{jkb}) (\sqrt{2} G_{0DL}^{*iks} - H_{0DR}^{*iks}) \left[G_{0ER}^{*jhl} G_{0ER}^{ihl} \right. \\ \left. \times G'(x_{\tilde{d}_k \tilde{\chi}_j^0}, x_{\tilde{l}_h \tilde{\chi}_j^0}, x_{\tilde{\chi}_i^0 \tilde{\chi}_j^0}) - 2 G_{0ER}^{*ihl} G_{0ER}^{jhl} \sqrt{x_{\tilde{\chi}_i^0 \tilde{\chi}_j^0}} F'(x_{\tilde{d}_k \tilde{\chi}_j^0}, x_{\tilde{l}_h \tilde{\chi}_j^0}, x_{\tilde{\chi}_i^0 \tilde{\chi}_j^0}) \right]. \quad (34)$$

The right handed supersymmetric contribution is

$$A_{\tilde{\chi}^-}^{R\Box} = \frac{\alpha_W^2}{4} \sum_{h,k=1}^6 \sum_{i,j=1}^5 \frac{1}{m_{\tilde{\chi}_i^-}^2} (G_{UR}^{jkb} - H_{UL}^{jkb}) (G_{UR}^{*iks} - H_{UL}^{*iks}) \\ \times G_{NR}^{*jhl} G_{NR}^{ihl} G'(x_{\tilde{u}_k \tilde{\chi}_j^-}, x_{\tilde{\nu}_h \tilde{\chi}_j^-}, x_{\tilde{\chi}_i^- \tilde{\chi}_j^-}), \quad (35)$$

$$A_{\tilde{\chi}^0}^{R\Box} = \frac{\alpha_W^2}{2} \sum_{i,j=1}^9 \sum_{k,h=1}^6 \frac{1}{m_{\tilde{\chi}_j^0}^2} (\sqrt{2} G_{0DR}^{jkb} - H_{0DL}^{jkb}) (\sqrt{2} G_{0DR}^{*iks} - H_{0DL}^{*iks}) \left[G_{0ER}^{*jhl} G_{0ER}^{ihl} \right. \\ \left. \times G'(x_{\tilde{d}_k \tilde{\chi}_j^0}, x_{\tilde{l}_h \tilde{\chi}_j^0}, x_{\tilde{\chi}_i^0 \tilde{\chi}_j^0}) - 2 G_{0ER}^{*ihl} G_{0ER}^{jhl} \sqrt{x_{\tilde{\chi}_i^0 \tilde{\chi}_j^0}} F'(x_{\tilde{d}_k \tilde{\chi}_j^0}, x_{\tilde{l}_h \tilde{\chi}_j^0}, x_{\tilde{\chi}_i^0 \tilde{\chi}_j^0}) \right], \quad (36)$$

$$A_{\tilde{\chi}^0}^{R\Box'} = -\frac{\alpha_W^2}{2} \sum_{i,j=1}^9 \sum_{k,h=1}^6 \frac{1}{m_{\tilde{\chi}_j^0}^2} (\sqrt{2} G_{0DR}^{jkb} - H_{0DL}^{jkb}) (\sqrt{2} G_{0DR}^{*iks} - H_{0DL}^{*iks}) \left[G_{0EL}^{*jhl} G_{0EL}^{ihl} \right. \\ \left. \times G'(x_{\tilde{d}_k \tilde{\chi}_j^0}, x_{\tilde{l}_h \tilde{\chi}_j^0}, x_{\tilde{\chi}_i^0 \tilde{\chi}_j^0}) - 2 G_{0EL}^{*ihl} G_{0EL}^{jhl} \sqrt{x_{\tilde{\chi}_i^0 \tilde{\chi}_j^0}} F'(x_{\tilde{d}_k \tilde{\chi}_j^0}, x_{\tilde{l}_h \tilde{\chi}_j^0}, x_{\tilde{\chi}_i^0 \tilde{\chi}_j^0}) \right]. \quad (37)$$

All the relevant vertex and loop functions are listed in the Appendix.

3.4 Branching ratios and asymmetries

Putting all the above contributions together, we write the total amplitude at the M_W scale as

$$\begin{aligned}\mathcal{A}_{tot}(M_W) &= C_7(M_W)Q_7 + \tilde{C}_7(M_W)\tilde{Q}_7 + C_9(M_W)Q_9 + \tilde{C}_9(M_W)\tilde{Q}_9 \\ &+ C_{10}(M_W)Q_{10} + \tilde{C}_{10}(M_W)\tilde{Q}_{10},\end{aligned}\tag{38}$$

where

$$\begin{aligned}\mathcal{A}_{tot}(M_W) &= C_7(M_W)Q_7 + \tilde{C}_7(M_W)\tilde{Q}_7 + C_9(M_W)Q_9 + \tilde{C}_9(M_W)\tilde{Q}_9 \\ &+ C_{10}(M_W)Q_{10} + \tilde{C}_{10}(M_W)\tilde{Q}_{10},\end{aligned}\tag{39}$$

where

$$C_7(M_W) = A_{LR}^\gamma,\tag{40}$$

$$\tilde{C}_7(M_W) = A_{RL}^\gamma,\tag{41}$$

$$C_9(M_W) = A_{LL}^\gamma + \left(-\frac{1}{4} + \sin^2 \theta_W\right)A^{Z_L} + \frac{1}{2} \left(A_{SM}^\square + A_{\tilde{\chi}^-}^{L\square} + A_{\tilde{\chi}^0}^{L\square} + A_{\tilde{\chi}^0}^{L\square'}\right),\tag{42}$$

$$\tilde{C}_9(M_W) = A_{RR}^\gamma + \frac{1}{2}(1 + \sin^2 \theta_W)A^{Z_R} + \frac{1}{2} \left(A_{\tilde{\chi}^-}^{R\square} + A_{\tilde{\chi}^0}^{R\square} + A_{\tilde{\chi}^0}^{R\square'}\right),\tag{43}$$

$$C_{10}(M_W) = \frac{1}{2}A^{Z_L} - \frac{1}{2} \left(A_{SM}^\square + A_{\tilde{\chi}^-}^{L\square} + A_{\tilde{\chi}^0}^{L\square} - A_{\tilde{\chi}^0}^{L\square'}\right),\tag{44}$$

$$\tilde{C}_{10}(M_W) = \sin^2 \theta_W A^{Z_R} + \frac{1}{2} \left(A_{\tilde{\chi}^-}^{R\square} + A_{\tilde{\chi}^0}^{R\square} - A_{\tilde{\chi}^0}^{R\square'}\right),\tag{45}$$

with

$$A_{LL}^\gamma = A_{SM}^{LL} + A_{H^-}^{LL} + A_{\tilde{g}}^{LL} + A_{\tilde{\chi}^-}^{LL} + A_{\tilde{\chi}^0}^{LL},\tag{46}$$

$$A_{RR}^\gamma = A_{\tilde{g}}^{RR} + A_{\tilde{\chi}^-}^{RR} + A_{\tilde{\chi}^0}^{RR},\tag{47}$$

$$A_{LR}^\gamma = A_{SM}^{LR} + A_{H^-}^{LR} + A_{\tilde{g}}^{LR} + A_{\tilde{\chi}^-}^{LR} + A_{\tilde{\chi}^0}^{LR},\tag{48}$$

$$A_{RL}^\gamma = A_{\tilde{g}}^{RL} + A_{\tilde{\chi}^-}^{RL} + A_{\tilde{\chi}^0}^{RL},\tag{49}$$

$$A^{Z_L} = A_{SM}^{Z_L} + A_{H^-}^{Z_L} + A_{\tilde{g}}^{Z_L} + A_{\tilde{\chi}^-}^{Z_L} + A_{\tilde{\chi}^0}^{Z_L},\tag{50}$$

$$A^{Z_R} = A_{\tilde{g}}^{Z_R} + A_{\tilde{\chi}^-}^{Z_R} + A_{\tilde{\chi}^0}^{Z_R}.\tag{51}$$

As the experimental results on semileptonic decays $B \rightarrow X_s l^+ l^-$ fit the SM well, new physics effects can be parameterized by R_i and \tilde{R}_i defined at the electroweak scale as

$$R_i = \frac{C_i - C_i^{SM}}{C_i^{SM}}, \quad \tilde{R}_i = \frac{\tilde{C}_i}{C_i^{SM}}. \quad (52)$$

Note that there are no contributions to \tilde{C}_i in the SM. The non-resonant branching ratios can be expressed in terms of the parameterization as [5]

$$\begin{aligned} \text{BR}(B \rightarrow X_s e^+ e^-) &= 7.29 \times 10^{-6} [1 + 0.35 R_7 + 0.179 R_9 + 0.714 R_{10} \\ &\quad + 0.0947(R_7^2 + \tilde{R}_7^2) + 0.045(R_9^2 + \tilde{R}_9^2) + 0.357(R_{10}^2 + \tilde{R}_{10}^2) \\ &\quad - 0.0313(R_7 R_9 + \tilde{R}_7 \tilde{R}_9)], \end{aligned} \quad (53)$$

$$\begin{aligned} \text{BR}(B \rightarrow X_s \mu^+ \mu^-) &= 4.89 \times 10^{-6} [1 + 0.0982 R_7 + 0.264 R_9 + 1.07 R_{10} \\ &\quad + 0.0491(R_7^2 + \tilde{R}_7^2) + 0.0671(R_9^2 + \tilde{R}_9^2) + 0.535(R_{10}^2 + \tilde{R}_{10}^2) \\ &\quad - 0.0467(R_7 R_9 + \tilde{R}_7 \tilde{R}_9)]. \end{aligned} \quad (54)$$

If R_i and \tilde{R}_i are set to zero, the SM values for the semileptonic decays are recovered in these formulas. Resonant contributions were studied in Ref. [15] and these can be avoided by excluding some special areas from the phase integration regions in the dilepton invariant mass.

We also consider the lepton pair energy asymmetry in the decay $B \rightarrow X_s l^+ l^-$ defined as

$$\mathcal{A}_{l^+ l^-} = \frac{N(E_{l^-} > E_{l^+}) - N(E_{l^+} > E_{l^-})}{N(E_{l^-} > E_{l^+}) + N(E_{l^+} > E_{l^-})}, \quad (55)$$

where, for instance, $N(E_{l^-} > E_{l^+})$ is the number of the lepton pairs where the negative charged lepton is more energetic than the positive charged lepton in the B rest frame. The energy asymmetry is equivalent to the

ordinary forward-backward asymmetry. In a configuration where l^+ is scattered in the forward direction, kinematically, in the dilepton center-of-mass frame, it is implied that $E_{l^+} < E_{l^-}$ in the B rest frame. With the above parameterization, the energy asymmetry is found to be

$$\begin{aligned} \mathcal{A}_{l^+l^-} = & \frac{0.48 \times 10^{-6}}{R_{\text{BR}}(\text{B} \rightarrow \text{X}_s l^+ l^-)} [1 - 0.625 R_7 + 0.884 R_9 + 0.911 R_{10} \\ & - 0.625 (R_7 R_{10} + \tilde{R}_7 \tilde{R}_{10}) + 0.884 (R_9 R_{10} + \tilde{R}_9 \tilde{R}_{10}) \\ & - 0.00882 (R_{10}^2 + \tilde{R}_{10}^2)], \end{aligned} \quad (56)$$

where $R_{\text{BR}}(\text{B} \rightarrow \text{X}_s l^+ l^-) = \frac{\text{BR}(\text{B} \rightarrow \text{X}_s l^+ l^-)}{\text{BR}(\text{B} \rightarrow \text{X}_s l^+ l^-)^{\text{SM}}}$.

4 Numerical Analysis

We are interested in analyzing the case in which the supersymmetric partners have masses around the weak scale, so we will assume relatively light superpartner masses. We diagonalize the neutralino, chargino, scalar quark and lepton mass matrices numerically and require in all calculations that the masses of gluinos, charginos, neutralinos, squarks and sleptons be above their experimental bounds. There are some extra constraints in the non-supersymmetric sector of the theory, requiring the FCNC Higgs boson Φ_d to be heavy, but no such constraints exist in the Higgsino sector [16]. We constrain the lightest Higgs boson mass to be 115 GeV [17].

As the first step, we assume the only source of flavor violation to come from the CKM matrix. This scenario is related to the minimal flavor violation case in supergravity. This restricted possibility of flavor violation will set important constraints on the parameter space of the LRSUSY model.

We then allow, in the second stage of our investigation, for new sources of flavor violation, coming from the soft breaking terms. In the MSSM, this

scenario is known as the unconstrained MSSM. We restrict all allowable LL, LR, RL and RR flavor mixings, assuming them to be dominated by mixings between the second and third squark family.

We now proceed to discuss both these scenarios in turn.

4.1 The constrained LRSUSY model

By the constrained LRSUSY model, we mean the scenario in which the only source of flavor violation comes from the quark sector, through the CKM matrix, which we assume to be the same for both the left- and right-handed sectors (manifest left-right symmetry), as explained below.

Before any meaningful numerical results be obtained, explicit values for the parameters in the model must be specified. There are many parameters in the model, such that it is hard, if not impossible, to get an illustrative presentation of calculation results. If the LRSUSY model is embedded in a supersymmetric grand unification theory such as $SO(10)$, there exist some relationships among the parameters at the unification scale M_{GUT} . We can generally choose specific values for parameters at the mass scale $\mu = M_{GUT}$, then use renormalization group equations to run them down to the low energy scale which is relevant to phenomenology. But, for maintaining both simplicity and generality, we can present an analysis in which the LRSUSY model is not embedded into another group. Then we can choose all parameters as independently free variables, with the numerical results confronting experimental bounds directly.

To make the results tractable, we assume all trilinear scalar couplings in the soft supersymmetry breaking Lagrangian as $A_{ij} = A\delta_{ij}$ and $\mu_{ij} = \mu\delta_{ij}$. We also set a common mass parameter for all the squarks $M_{0UL} =$

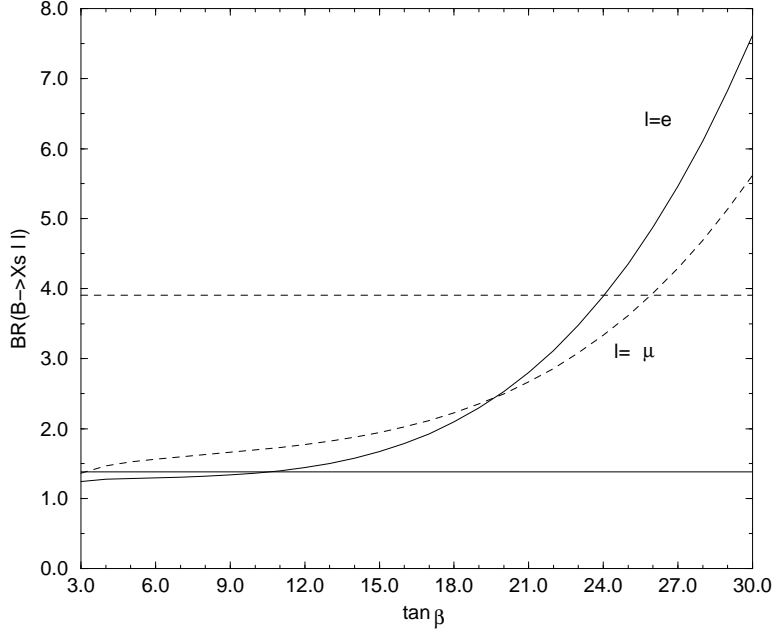


Figure 3: $\text{BR}(B \rightarrow X_s l^+ l^-)$ normalized to the corresponding SM values as a function of $\tan \beta$, obtained when $m_{\tilde{g}} = 300$ GeV, $\mu = 100$ GeV, $A=50$ GeV, $M_L = M_R = 500$ GeV, $m_{0q} = 300$ GeV and $m_{0l} = 100$ GeV. The experimental constraints are also shown.

$M_{0UR} = M_{0DL} = M_{0DR} = m_{0q}$. We take $K_{CKM}^L = K_{CKM}^R$. This choice is conservative, and much larger values of mixing matrix elements are allowed in scenarios that attempt to explain the decay properties of the b quark as being saturated by the right-handed b [6]. Our choice does not favor one handedness over the other, and has the added advantage that no new mixing angles are introduced in the quark matrices.

We investigate first the dependence of the branching ratio on the values of $\tan \beta$ in Fig. 3. The branching ratios are normalized to the corresponding SM values. In the whole parameter range, the branching ratio is greater than one, which means that large enhancements can be obtained in the LR-SUSY model with respect the SM. This feature is similar to the one in the MSSM and is due to the $1/\cos \beta$ enhancement in the chargino interaction vertices. For example, when $\tan \beta$ is around 30, an enhancement of one

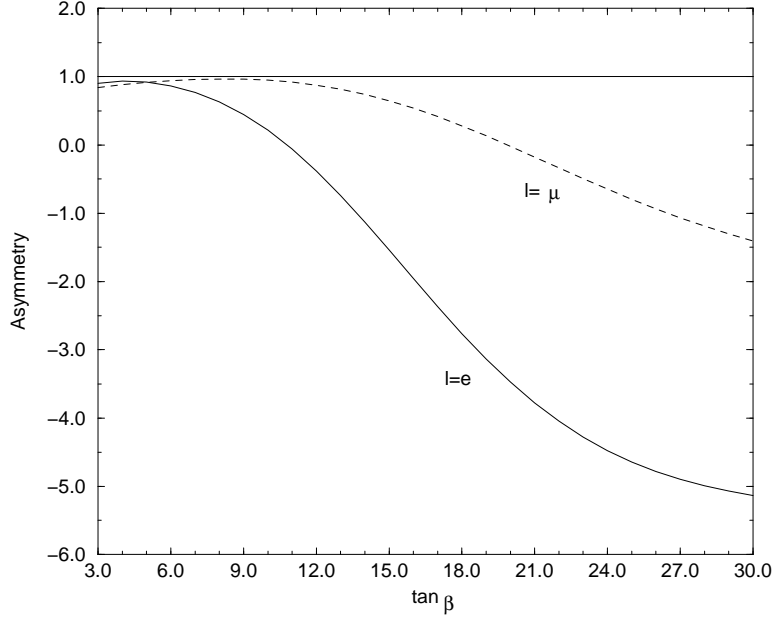


Figure 4: Energy asymmetry $A(B \rightarrow X_s l^+ l^-)$ normalized to the corresponding SM values as a function of $\tan \beta$, obtained when $m_{\tilde{g}} = 300$ GeV, $\mu = 100$ GeV, $A = 50$ GeV, $M_L = M_R = 500$ GeV, $m_{0q} = 300$ GeV and $m_{0l} = 100$ GeV.

order of magnitude can be obtained. This would make the rare semileptonic decay more easily to be observed in future experiments. Generally the branching ratio increases with $\tan \beta$, and for larger values of $\tan \beta$ the branching ratio will exceed the acceptable range easily. The choice of parameters puts stringent restrictions on the allowed values for $\tan \beta$. For the electron, $\tan \beta$ should be less than 11 if the branching ratio is to be below the experimental bounds, while for the muon $\tan \beta$ should be less than 26, mainly due to the experimental bound of the muon is larger than that of the electron. The asymmetries corresponding to different values of $\tan \beta$ are shown in Fig. 4. A clear deviation from the SM model is also obtained. Note that in the SM the asymmetry is normalized to 1. The asymmetries tend to be large and negative with increasing $\tan \beta$.

We investigate next the dependence of the branching ratio and asym-

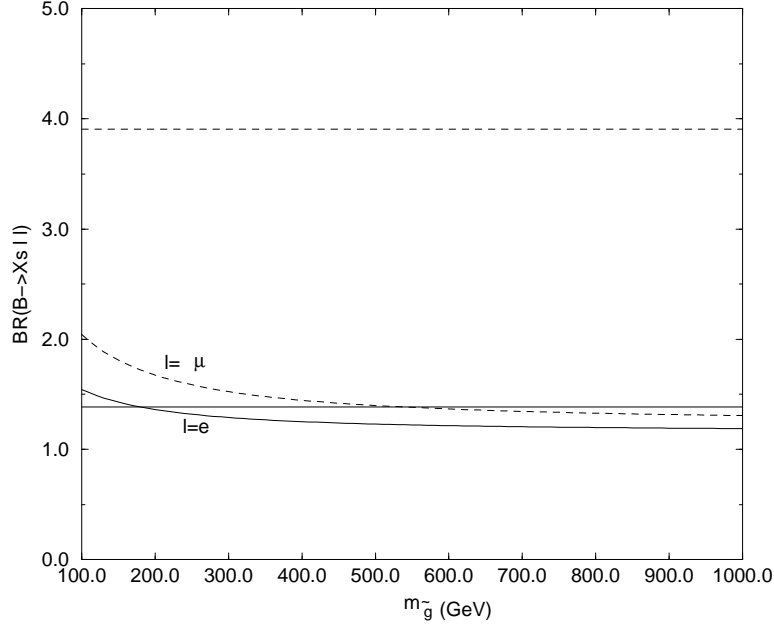


Figure 5: $\text{BR}(B \rightarrow X_s l^+ l^-)$ normalized to the corresponding SM values as a function of $m_{\tilde{g}}$, obtained when $\tan \beta = 5$, $\mu = 100$ GeV, $A = 50$ GeV, $M_L = M_R = 500$ GeV, $m_{0q} = 300$ GeV and $m_{0l} = 100$ GeV. The experimental constraints are also shown.

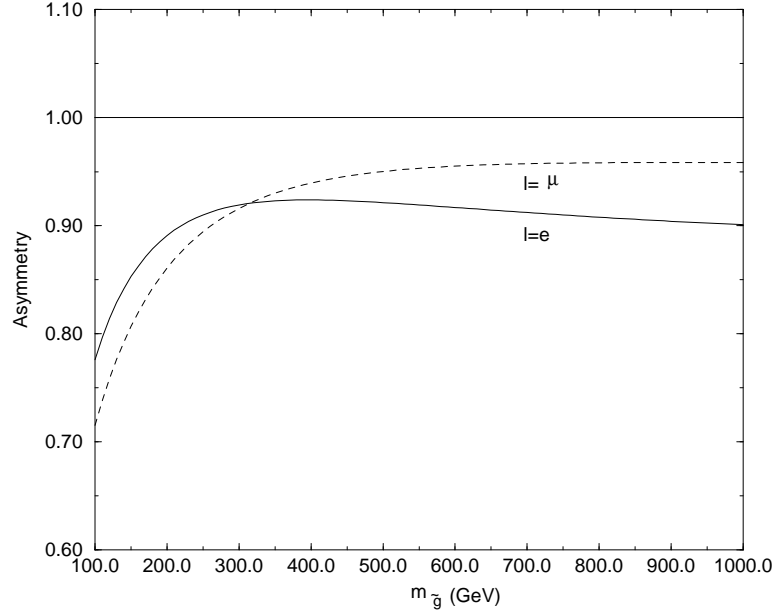


Figure 6: Energy asymmetry $A(B \rightarrow X_s l^+ l^-)$ normalized to the corresponding SM values as a function of $m_{\tilde{g}}$, obtained when $\tan \beta = 5$, $\mu = 100$ GeV, $A = 50$ GeV, $M_L = M_R = 500$ GeV, $m_{0q} = 300$ GeV and $m_{0l} = 100$ GeV.

metry on the gluino mass, for a light squark scenario. The chargino and neutralino masses are light and $\mu > 0$, a scenario favored by recent analyses of the anomalous magnetic moment of the muon [18] and consistent with $b \rightarrow s\gamma$ [1]. We present the results in Fig. 5. As the mass of gluino increases, the branching ratio will decrease, as the gluino is exchanged as a virtual particle in the process. From the branching ratio into electrons, the gluino mass is constrained to be heavier than 200 GeV, which is weaker than other constraints, for example, from $b \rightarrow s\gamma$; while from the muon case there is no constraint on $m_{\tilde{g}}$. Therefore in the LRSUSY model the contributions from gluino-exchanged graphs are not dominant, while this is generally so in $b \rightarrow s\gamma$. The corresponding asymmetries are shown in Fig. 6. It is found that the asymmetries for both the electron and muon are less than the corresponding SM value. Although asymmetries do not help the experimentalists to observe the decay, they might, if observed, serve to distinguish the LRSUSY model from the SM.

The branching ratio of $B \rightarrow X_s l^+ l^-$ is sensitive to the universal scalar mass m_{0q} in the region of small masses only, a feature shared with $b \rightarrow s\gamma$ [1]. This dependence is shown in Fig. 7. For the electron case, m_{0q} is found to be greater than 200 GeV, where the corresponding scalar quark masses are slightly above the current experimental bounds, while for muon case there is no constraint on m_{0q} . The lepton asymmetries as a function of the universal scalar mass, are shown in Fig. 8, and there a small enhancement can be found when m_{0q} is less than 300 GeV.

In all the previous figures we set the left- and right-handed gaugino masses to the same value. In Fig. 9 and Fig. 10 we investigate the dependence of the branching ratios and asymmetries on the gaugino mass.

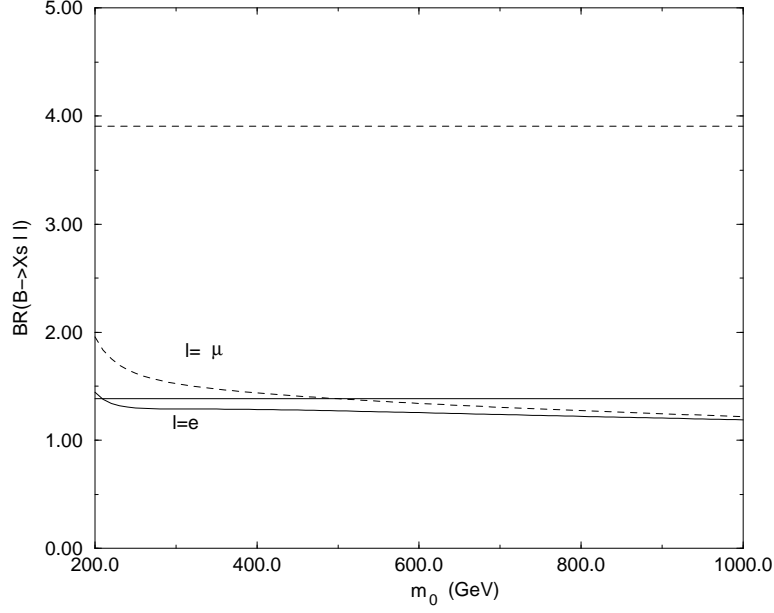


Figure 7: $\text{BR}(B \rightarrow X_s l^+ l^-)$ normalized to the corresponding SM values as a function of m_0 , obtained when $m_{\tilde{g}} = 300$ GeV, $\tan \beta = 5$, $\mu = 100$ GeV, $A = 50$ GeV, $M_L = M_R = 500$ GeV and $m_{0l} = 100$ GeV. The experimental constraints are also shown.

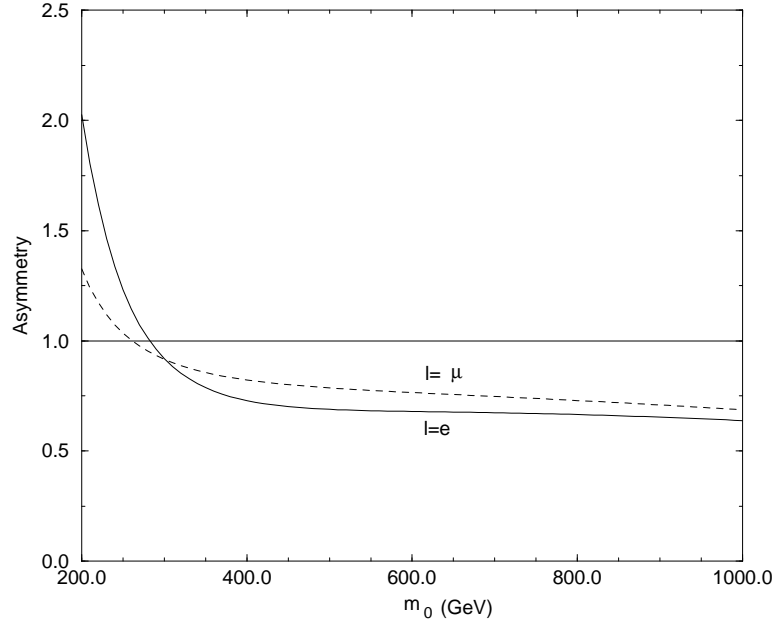


Figure 8: Energy asymmetry $A(B \rightarrow X_s l^+ l^-)$ normalized to the corresponding SM values as a function of m_0 , $\tan \beta = 5$, obtained when $m_{\tilde{g}} = 300$ GeV, $\mu = 100$ GeV, $A = 50$ GeV, $M_L = M_R = 500$ GeV and $m_{0l} = 100$ GeV.

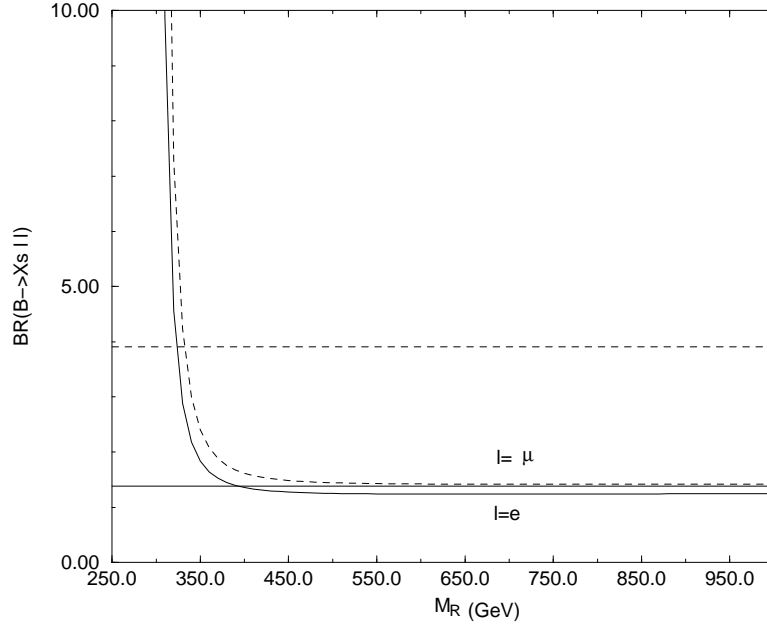


Figure 9: $\text{BR}(B \rightarrow X_s l^+ l^-)$ normalized to the corresponding SM values as a function of M_R , obtained when $m_{\tilde{g}} = 400$ GeV, $\tan \beta = 5$, $\mu = 100$ GeV, $A=50$ GeV, $m_{0q} = 300$ GeV and $m_{0l} = 100$ GeV. The experimental constraints are also shown.

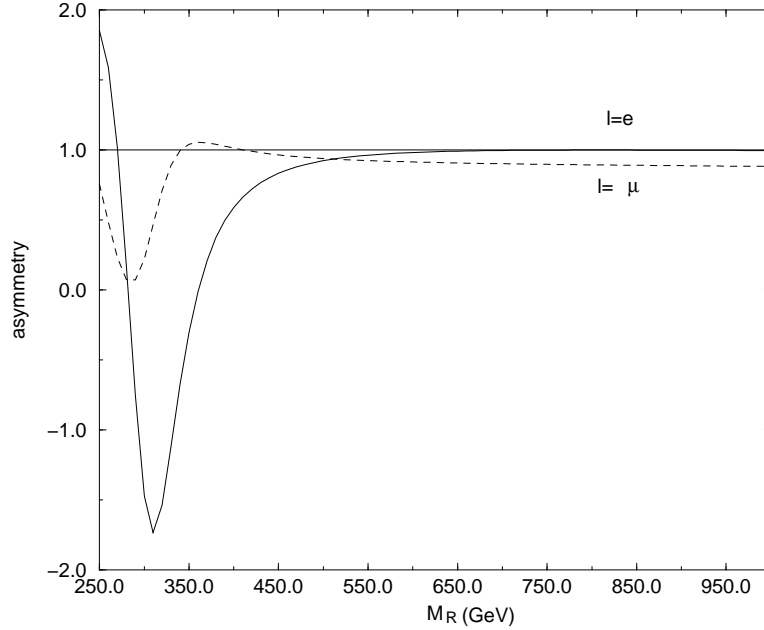


Figure 10: Energy asymmetry $A(B \rightarrow X_s l^+ l^-)$ normalized to the corresponding SM values as a function of M_R , obtained when $m_{\tilde{g}} = 400$ GeV, $\tan \beta = 5$, $\mu = 100$ GeV, $A=50$ GeV, $m_{0q} = 300$ GeV and $m_{0l} = 100$ GeV.

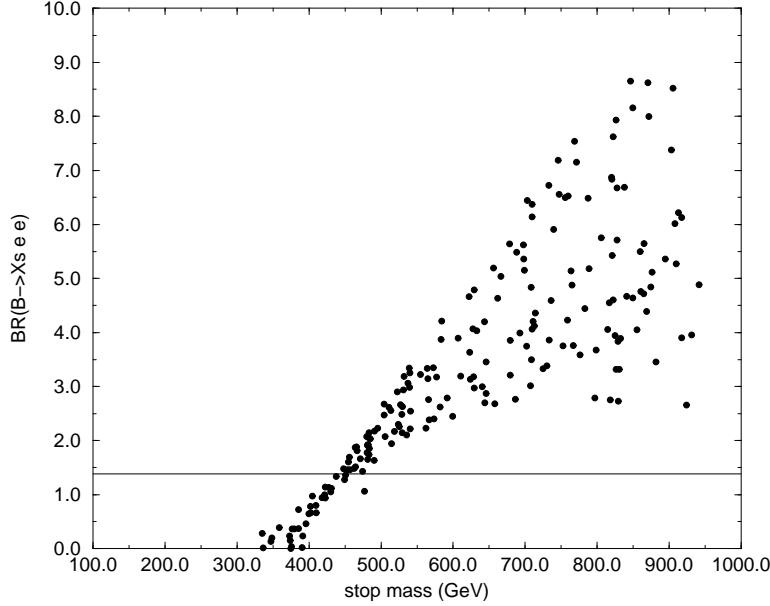


Figure 11: $\text{BR}(B \rightarrow X_s e^+ e^-)$ normalized to the corresponding SM values versus the lightest stop mass in the LRSUSY model.

When $M_R \cong m_{0q}$, the results are not reliable, due to poles in the loop functions. As the branching ratio of $B \rightarrow X_s l^+ l^-$ is dominated by the chargino contribution for a large region of the parameter space, one expects a restriction on the left- and right-handed gaugino mass parameters. There exist scenarios in which the right-handed symmetry is broken at the same scale as supersymmetry, so we expect in those cases to have approximately $M_L = M_R$ [19]. With the assumption $M_L \cong M_R$ in the gaugino sector, the restriction on the right-handed gaugino scale is found to be $M_R > 400 - 500$ GeV, for low to intermediate squark masses.

In Fig. 11 and Fig. 12 we present the scatter plots of the branching ratio and the asymmetry for the decay $B \rightarrow X_s e^+ e^-$ as a function of the lightest stop mass. We have chosen randomly relevant parameters: $\tan \beta$ changes from 2 to 30, m_{0q} takes values from 100 to 1000 GeV, μ also varies from 100 to 1000 GeV and $A = m_{0q}$, while $m_{\tilde{g}} = 500$ GeV, $M_L = M_R = 500$

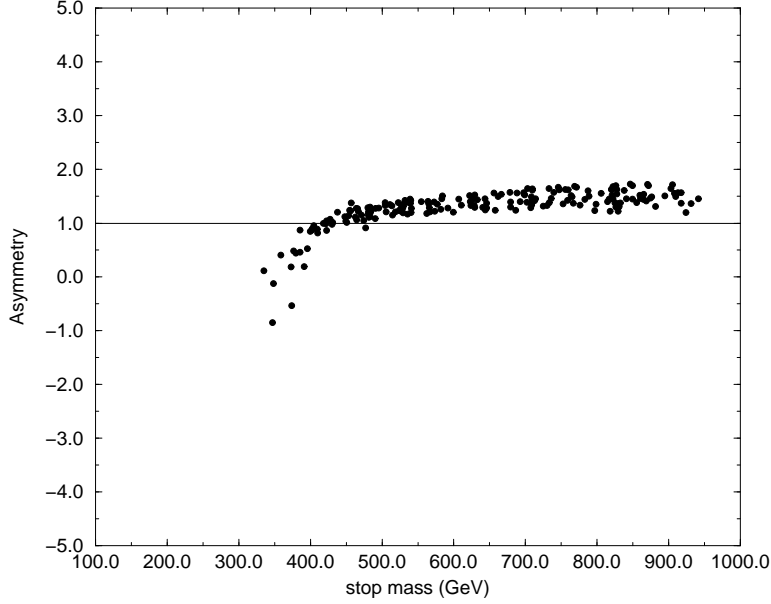


Figure 12: Energy asymmetry $A(B \rightarrow X_s e^+ e^-)$ normalized to the corresponding SM values versus the lightest stop mass in the LRSUSY model.

GeV and $m_{0t} = 100$ GeV. In addition to the current experimental bounds on the SUSY spectra, we also impose the constraints from the rare decay $b \rightarrow s\gamma$. It is found that the lightest stop masses lower than 300 GeV are excluded. The branching ratio fits easily within the experimental bound for large $m_{\tilde{t}}$, which explains the large number of plot points in that region. An enhancement for the branching ratio of one order of magnitude is possible while the asymmetry could be 50% larger than the SM value.

In Fig. 13 we show the correlation between the branching ratio of the $b \rightarrow s\gamma$ and $B \rightarrow X_s e^+ e^-$ in the above specified parameter ranges. Both branching ratios are normalized to the corresponding SM values. Although it seems possible that $b \rightarrow s\gamma$ is below the SM value, while $B \rightarrow X_s e^+ e^-$ is enhanced with respect to the SM value, there exists a region of the parameter space in which both are significantly enhanced with respect to their SM values.

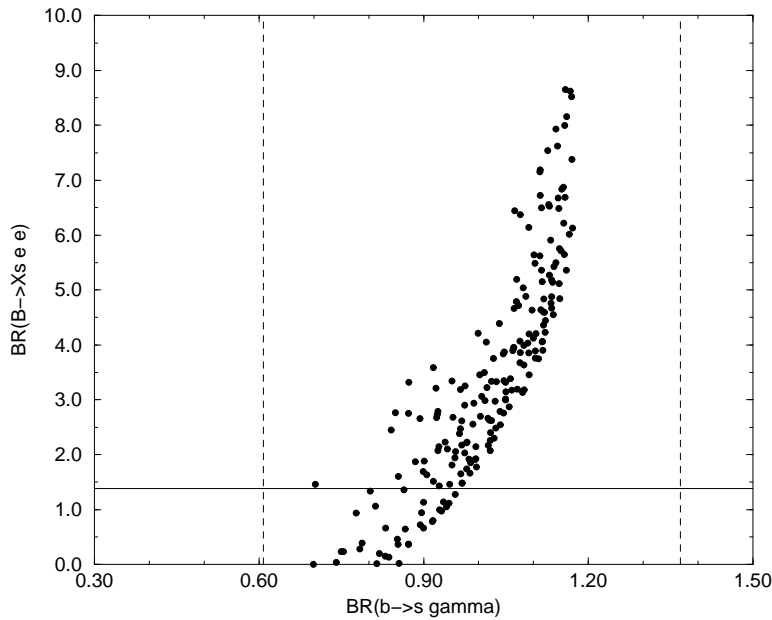


Figure 13: A correlation between $\text{BR}(b \rightarrow s\gamma)$ and $\text{BR}(B \rightarrow X_s e^+ e^-)$ in the LRSUSY model. Experimental bounds are also shown.

4.2 The unconstrained LRSUSY model

When supersymmetry is softly broken, there is no reason to expect that the soft parameters would be flavor blind, or that they would violate flavor in the same way as in the SM. Yukawa couplings generally form a matrix in the generation space, and the off-diagonal elements will lead naturally to flavor changing radiative decays. Neutrino oscillations, in particular, indicate strong flavor mixing between the second and third neutrino generations, and various analyses have been carried out assuming the same for the charged sleptons. In the quark/squark sector, the kaon system strongly limits mixings between the first and the second generations; constraints for the third generation from $b \rightarrow s\gamma$ in the LRSUSY model are studied in Ref. [1].

We parametrize all the unknown soft breaking parameters, coming mostly

from the scalar mass matrices, using the mass insertion approximation (MI) [20]. In this framework we choose a basis for fermion and sfermion states in which all the couplings of these particles to neutral gauginos are flavor diagonal. Flavor changes in the squark sector arise from the non-diagonality of the squark propagators. These off-diagonal squark mass matrix elements are assumed to be small and their higher orders can be neglected, and the normalized parameters used in the analysis are:

$$\begin{aligned}\delta_{d,LL,ij} &= \frac{(m_{d,LL}^2)_{ij}}{m_{0q}^2}, & \delta_{d,RR,ij} &= \frac{(m_{d,RR}^2)_{ij}}{m_{0q}^2}, \\ \delta_{d,LR,ij} &= \frac{(m_{d,LR}^2)_{ij}}{m_{0q}^2}, & \delta_{d,RL,ij} &= \frac{(m_{d,RL}^2)_{ij}}{m_{0q}^2},\end{aligned}\tag{57}$$

where $(m_{d,AB}^2)_{ij}$, $A, B = L, R$ are the off-diagonal elements which mix down-squark flavors for both left- and right-handed squarks. We assume significant mixings between the second and third generation in the down-squarks mass matrix only. We also consider terms with one mass insertion only. Although it was shown in the MSSM that double mass insertions could possibly enhance the decays of the K meson, their effects on B meson decays are assumed to be negligible. This procedure allows an analysis of the graphs contributing to $b \rightarrow sl^+l^-$ in terms of a small number of parameters. The contribution of each graph with the MI is obtained from the constrained case following these simple rules:

- A left gaugino-gaugino vertex has a factor of $\delta_{d,LL,23}$ associated with it; a right gaugino-gaugino vertex has a factor of $\delta_{d,RR,23}$.
- A left gaugino Higgsino vertex has a factor of $\delta_{d,LR,23}$ associated with it; a right gaugino-Higgsino vertex has a factor of $\delta_{d,RL,23}$.

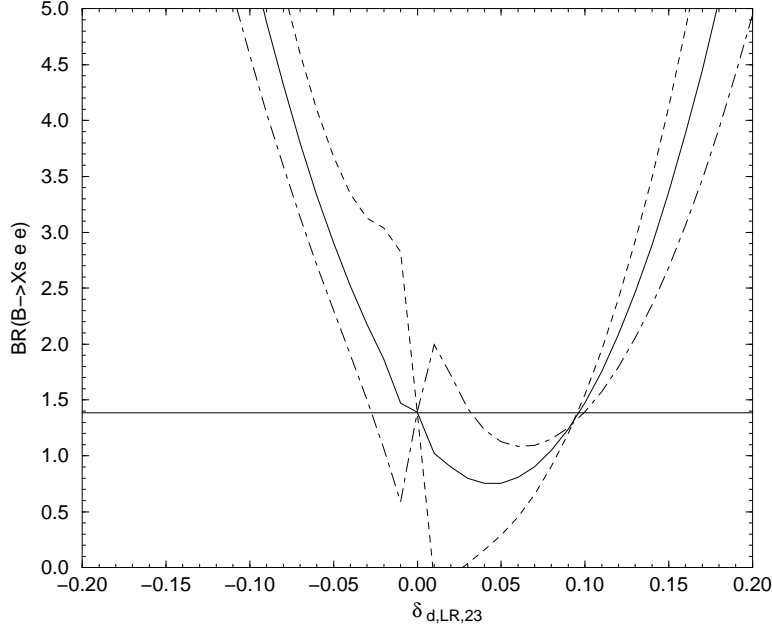


Figure 14: $\text{BR}(B \rightarrow X_s e^+ e^-)$ normalized to the corresponding SM values as a function of $\delta_{d,LR,23}$, obtained when $\tan \beta = 5$, $\mu = 100$ GeV, $A = 50$ GeV, $M_L = M_R = 500$ GeV, $m_{0q} = 500$ GeV and $m_{0l} = 100$ GeV. The different lines correspond to different values of $x = m_{\tilde{g}}^2/m_{0q}^2 = 0.64$ (*dashed*), 1 (*solid*), 1.44 (*dot - dashed*). The experimental constraints are also shown.

- In addition, in the dipole contributions, the term coming from chirality being flipped on the fermion leg, proportional to $m_{\tilde{\chi}}/m_b$ or $m_{\tilde{g}}/m_b$, has a factor $\delta_{d,LR,23}$ associated with it for the LR contribution, and $\delta_{d,RL,23}$ associated with it for the RL contribution.

With the definition of the mass insertion as in Eq. (57), we can investigate the effects of intergenerational mixings on the $B \rightarrow X_s l^+ l^-$ decays. We keep our analysis general, but to show our results, we select only one possible source of flavor violation in the squark sector at a time, and assume the others vanish. In Fig. 14 we show the dependence of $B \rightarrow X_s e^+ e^-$ as a function of $\delta_{d,LR,23}$, when this is the only source of flavor violation. The horizontal line represents the experimental bound on the branching ratio.

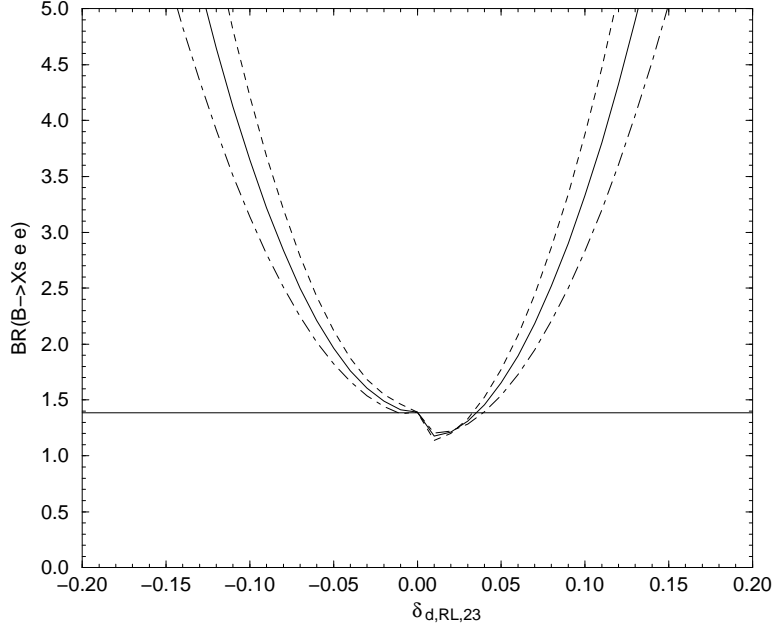


Figure 15: $\text{BR}(B \rightarrow X_s e^+ e^-)$ normalized to the corresponding SM values as a function of $\delta_{d,LR,23}$, obtained when $\tan \beta = 5$, $\mu = 100$ GeV, $A = 50$ GeV, $M_L = M_R = 500$ GeV, $m_{0q} = 500$ GeV and $m_{0l} = 100$ GeV. The different lines correspond to different values of $x = m_g^2/m_{0q}^2 = 0.64$ (*dashed*), 1 (*solid*), 1.44 (*dot - dashed*). The experimental constraints are also shown.

The branching ratio is plotted as a function of different values for the mass ratio $x = m_g^2/m_{0q}^2$. Fixing $m_{0q} = 500$ GeV, this corresponds to gluino masses of 400, 500 and 600 GeV respectively. Constraints on positive and negative values of $\delta_{d,LR,23}$ are slightly different, $\delta_{d,LR,23}$ is constrained to be positive for small mass ratios, and the absolute value of $\delta_{d,LR,23}$ is less than 10%. This flavor violating parameter can be strongly constrained from $b \rightarrow s\gamma$ because through the $\delta_{d,LR,23}$ term, the helicity flip needed for $b \rightarrow s\gamma$ can be realized in the exchange particle loop. The constraint obtained here is complimentary to that from $b \rightarrow s\gamma$ [1, 21, 22]. The results for $B \rightarrow X_s \mu^+ \mu^-$ are not restrictive, so we will not show them here.

The situation is different when the only source of flavor violation is $\delta_{d,RL,23}$, as shown in Fig. 15. Again, the most restrictive case is for $B \rightarrow$

$X_s e^+ e^-$ and for the same values of squark and gluino masses as before, only positive values of $\delta_{d,RL,23}$ in a small interval close to zero would satisfy the experimental bounds, namely $\delta_{d,RL,23} < 4\%$.

The restrictions on the branching ratio of $B \rightarrow X_s l^+ l^-$ from the chirality conserving mixings $\delta_{d,LL,23}$ and $\delta_{d,RR,23}$ respectively, with the proviso that these are the only off-diagonal matrix elements in the squark mass matrix squared, are not as pronounced as the ones for chirality flipping parameters. $\delta_{d,LL,23}$ and $\delta_{d,RR,23}$ can almost take all the values in the range $(-1.0, 1.0)$. We don't show the results here.

5 Conclusions

We analyze the FCNC semileptonic decay $B \rightarrow X_s l^+ l^-$ in a fully left-right supersymmetric model. Explicit expressions for all the amplitudes involved in the process are given. Constraints on the parameter space of the model are obtained in both the constrained case (where the only flavor violation comes from the CKM matrix) and the unconstrained case (including soft supersymmetry breaking terms). We also include and compare with constraints from $b \rightarrow s\gamma$.

As a general feature, both $b \rightarrow s\gamma$ and $B \rightarrow X_s l^+ l^-$ exhibit similar dependences on squark and gluino masses. From restrictions on both decays, we expect $m_{\tilde{g}} \geq 250 - 300$ GeV and $m_{\tilde{q}} \geq 200$ GeV. A more careful analysis of the branching ratio of $B \rightarrow X_s l^+ l^-$ reveals that, varying all other parameters in the model, the mass of the lightest scalar top should be ≥ 300 GeV, which is much more restrictive than the experimental bound [23]. The parameter that most sensitively affects the branching ratio of $B \rightarrow X_s l^+ l^-$

is $\tan\beta$. The constraint from $B \rightarrow X_s l^+ l^-$ is slightly more restrictive than for $b \rightarrow s\gamma$, and the semileptonic branching ratio can exceed the experimental bound for $\tan\beta \geq 10 - 11$, for low squark and gluino masses. In all our analysis, we keep $\mu > 0$, and in regions allowed by both $(g - 2)_\mu$ and $b \rightarrow s\gamma$.

An analysis of the correlation between the branching ratio of $B \rightarrow X_s \gamma$ and $B \rightarrow X_s l^+ l^-$ reveals that there is a larger region of parameter space in which $B \rightarrow X_s l^+ l^-$ is enhanced with respect to the SM value by factors of almost 10, while $B \rightarrow X_s \gamma$ is at most 20% larger than the SM value. We expect the enhancements to come mostly from regions of intermediate or large $\tan\beta$. The LRSUSY model shares the strong $\tan\beta$ dependence with the MSSM, except that here the enhancement is even more pronounced. The asymmetry also shows different features from the MSSM [24]: it does not peak when the Higgs and gauge induced flavor violation are of the same size ($\tan\beta = 35$), since the contributions from the gaugino sector are different. Also, for low and intermediate values of supersymmetric masses ($m_0, m_{\tilde{g}}, M_L, M_R = 200 - 500$ GeV), this value of $\tan\beta$ is ruled out by constraints from $B \rightarrow X_s e^+ e^-$.

In the unconstrained model, allowing for flavor-dependent soft mixing between the second and third generation of squarks (both chirality conserving and chirality violating), no reliable limits are set on either the LL or the RR mixing. However, the chirality violating soft mixing parameters are strongly constrained. In particular, the RL mixing, $\delta_{d,RL,23}$ is constrained within four percentage to be close to zero from the bounds on $B \rightarrow X_s e^+ e^-$, for a variety of squark and gluino masses; while the constraints on $\delta_{d,LR,23}$ favor positive values up to 10%. It could be difficult to compare these val-

ues with the unconstrained MSSM [25]. The bound on $\delta_{d,LR,23}$ appears to be much stronger in the unconstrained LRSUSY model than in the MSSM, where maximum enhancements are obtained at values of the left-right splitting ruled out in the LRSUSY model. And certainly the restriction on the $\delta_{d,RL,23}$ coming from $B \rightarrow X_s e^+ e^-$ is, to our knowledge, new.

It appears likely that the most distinguishing factor of the LRSUSY model from the SM would be the forward-backward lepton asymmetry. This asymmetry, like the branching ratio, is most sensitive to variations in $\tan \beta$ and could be spectacular even in regions of $\tan \beta$ allowed by constraints on the branching ratio. The asymmetry tends to be large and negative with increasing $\tan \beta$, whereas it is small and positive when varying other parameters. As always, the regions of interest are regions of small to intermediate values (allowed for branching ratios) for gluino, chargino and squark masses. These enhancements are much more pronounced in the LRSUSY model than in the MSSM, and increases in the asymmetry by a factor of 2 with respect to the SM value are allowed, for a large region of the parameter space.

In conclusion, the decay $B \rightarrow X_s l^+ l^-$ would provide an interesting, and complementary to $b \rightarrow s\gamma$, test of the LRSUSY model.

Acknowledgements

This work was funded by NSERC of Canada (SAP0105354).

Appendix

The relevant Feynman rules and loop functions used in the calculation are listed in this Appendix. For further details, we refer to [1]. The terms relevant to the masses of charginos in the Lagrangian are

$$\mathcal{L}_C = -\frac{1}{2}(\psi^+, \psi^-) \begin{pmatrix} 0 & X^T \\ X & 0 \end{pmatrix} \begin{pmatrix} \psi^+ \\ \psi^- \end{pmatrix} + H.c. , \quad (58)$$

where $\psi^+ = (-i\lambda_L^+, -i\lambda_R^+, \tilde{\phi}_{u1}^+, \tilde{\phi}_{d1}^+, \tilde{\Delta}_R^+)^T$ and $\psi^- = (-i\lambda_L^-, -i\lambda_R^-, \tilde{\phi}_{u2}^-, \tilde{\phi}_{d2}^-, \tilde{\delta}_R^-)^T$,

and

$$X = \begin{pmatrix} M_L & 0 & g_L \kappa_u & 0 & 0 \\ 0 & M_R & g_R \kappa_u & 0 & 0 \\ 0 & 0 & 0 & -\mu & 0 \\ g_L \kappa_d & g_R \kappa_d & -\mu & 0 & 0 \\ 0 & \sqrt{2} g_R v_R & 0 & 0 & -\mu \end{pmatrix} \quad (59)$$

where we have taken, for simplification, $\mu_{ij} = \mu$. The chargino mass eigenstates χ_i are obtained by

$$\chi_i^+ = V_{ij} \psi_j^+, \quad \chi_i^- = U_{ij} \psi_j^-, \quad i, j = 1, \dots, 5, \quad (60)$$

with V and U unitary matrices satisfying

$$U^* X V^{-1} = M_D, \quad (61)$$

The diagonalizing matrices U^* and V are obtained by computing the eigenvectors corresponding to the eigenvalues of $X^\dagger X$ and XX^\dagger , respectively.

The terms relevant to the masses of neutralinos in the Lagrangian are

$$\mathcal{L}_N = -\frac{1}{2} \psi^{0T} Y \psi^0 + H.c. , \quad (62)$$

where $\psi^0 = (-i\lambda_L^3, -i\lambda_R^3, -i\lambda_V, \tilde{\phi}_{u1}^0, \tilde{\phi}_{u2}^0, \tilde{\phi}_{d1}^0, \tilde{\phi}_{d2}^0, \tilde{\Delta}_R^0, \tilde{\delta}_R^0)^T$, and

$$Y = \begin{pmatrix} M_L & 0 & 0 & \frac{g_L \kappa_u}{\sqrt{2}} & 0 & 0 & -\frac{g_L \kappa_d}{\sqrt{2}} & 0 & 0 \\ 0 & M_R & 0 & \frac{g_R \kappa_u}{\sqrt{2}} & 0 & 0 & -\frac{g_R \kappa_d}{\sqrt{2}} & -\sqrt{2}g_R v_R & 0 \\ 0 & 0 & M_V & 0 & 0 & 0 & 0 & 2\sqrt{2}g_V v_R & 0 \\ \frac{g_L \kappa_u}{\sqrt{2}} & \frac{g_R \kappa_u}{\sqrt{2}} & 0 & 0 & 0 & 0 & -\mu & 0 & 0 \\ 0 & 0 & 0 & 0 & 0 & -\mu & 0 & 0 & 0 \\ 0 & 0 & 0 & 0 & -\mu & 0 & 0 & 0 & 0 \\ -\frac{g_L \kappa_d}{\sqrt{2}} & -\frac{g_R \kappa_d}{\sqrt{2}} & 0 & -\mu & 0 & 0 & 0 & 0 & 0 \\ 0 & -\sqrt{2}g_R v_R & \sqrt{2}g_V v_R & 0 & 0 & 0 & 0 & 0 & -\mu \\ 0 & 0 & 0 & 0 & 0 & 0 & 0 & -\mu & 0 \end{pmatrix}. \quad (63)$$

The mass eigenstates are defined by

$$\chi_i^0 = N_{ij}\psi_j^0 \quad (i, j = 1, 2, \dots, 9), \quad (64)$$

where N is a unitary matrix chosen such that

$$N^* Y N^{-1} = N_D, \quad (65)$$

and N_D is a diagonal matrix with non-negative entries.

In the interaction basis, $(\tilde{q}_L^i, \tilde{q}_R^i)$, the squared-mass matrix for a squark of flavor f has the following forms. For U-type squarks

$$\mathcal{M}_{U_k}^2 = \begin{pmatrix} m_0^2 + M_Z^2(T_u^3 - Q_u \sin^2 \theta_W) \cos 2\beta & m_{u_k}(A - \mu \cot \beta) \\ m_{u_k}(A - \mu \cot \beta) & m_0^2 + M_Z^2 Q_u \sin^2 \theta_W \cos 2\beta \end{pmatrix}. \quad (66)$$

and for D-type squarks

$$\mathcal{M}_{D_k}^2 = \begin{pmatrix} m_0^2 + M_Z^2(T_d^3 - Q_d \sin^2 \theta_W) \cos 2\beta & m_{d_k}(A - \mu \tan \beta) \\ m_{d_k}(A - \mu \tan \beta) & m_0^2 + M_Z^2 Q_d \sin^2 \theta_W \cos 2\beta \end{pmatrix}. \quad (67)$$

The corresponding mass eigenstates are defined as

$$\tilde{q}_{L,R} = \Gamma_{Q \ L,R}^\dagger \tilde{q}, \quad (68)$$

where $\Gamma_{Q \ L,R}^\dagger$ are 6×3 mixing matrices. The same expressions, with the switches $Q \rightarrow L$, $U \rightarrow N$ and $D \rightarrow E$ exist for the sleptons and sneutrinos.

The chargino-quark-squark mixing matrices G and H are defined as

$$\begin{aligned}
G_{UL}^{jki} &= V_{j1}^* (K_{CKM})_{il} (\Gamma_{UL})_{kl}, \\
G_{UR}^{jki} &= U_{j2} (K_{CKM})_{il} (\Gamma_{UR})_{kl}, \\
H_{UL}^{jki} &= \frac{1}{\sqrt{2}m_W} \left(\frac{m_{u_l}}{\sin \beta} U_{j3} + \frac{m_{d_l}}{\cos \beta} U_{j4} \right) (K_{CKM})_{il} (\Gamma_{UL})_{kl}, \\
H_{UR}^{jki} &= \frac{1}{\sqrt{2}m_W} \left(\frac{m_{u_l}}{\sin \beta} V_{j3}^* + \frac{m_{d_l}}{\cos \beta} V_{j4}^* \right) (K_{CKM})_{il} (\Gamma_{UR})_{kl}.
\end{aligned} \tag{69}$$

and the gaugino-sneutrino-lepton $G_{NL,R}$ are defined as

$$G_{NL,R}^{jki} = V_{j1}^* (\Gamma_{NL,R})_{ki}. \tag{70}$$

The neutralino-quark-squark mixing matrices G_0 and H_0 are defined as

$$\begin{aligned}
G_{0DL}^{jki} &= [\sin \theta_W Q_d N'_{j1} + \frac{1}{\cos \theta_W} (T_d^3 - Q_d \sin^2 \theta_W) N'_{j2} \\
&\quad - \frac{\sqrt{\cos 2\theta_W}}{\cos \theta_W} \frac{Q_u + Q_d}{2} N'_{j3}] (K_{CKM})_{il} (\Gamma_{DL})_{kl}, \\
G_{0DR}^{jki} &= -[\sin \theta_W Q_d N'_{j1} - \frac{Q_d \sin^2 \theta_W}{\cos \theta_W} N'_{j2} \\
&\quad + \frac{\sqrt{\cos 2\theta_W}}{\cos \theta_W} (T_d^3 - Q_d \sin^2 \theta_W) N'_{j3}] (K_{CKM})_{il} (\Gamma_{DR})_{kl}, \\
H_{0DL}^{jki} &= \frac{1}{\sqrt{2}m_W} \left(\frac{m_{u_l}}{\sin \beta} N'_{j5} + \frac{m_{d_l}}{\cos \beta} N'_{j7} \right) (K_{CKM})_{il} (\Gamma_{DL})_{kl}, \\
H_{0DR}^{jki} &= \frac{1}{\sqrt{2}m_W} \left(\frac{m_{u_l}}{\sin \beta} N'_{j5}^* + \frac{m_{d_l}}{\cos \beta} N'_{j7}^* \right) (K_{CKM})_{il} (\Gamma_{DR})_{kl}.
\end{aligned} \tag{71}$$

and the gaugino-slepton-lepton mixing matrices G_{0EL} , G_{0ER} are defined as

$$\begin{aligned}
G_{0EL}^{jki} &= [\sin \theta_W Q_e N'_{j1} + \frac{1}{\cos \theta_W} (T_e^3 - Q_e \sin^2 \theta_W) N'_{j2} \\
&\quad - \frac{\sqrt{\cos 2\theta_W}}{\cos \theta_W} \frac{Q_e}{2} N'_{j3}] (\Gamma_{EL})_{ki}, \\
G_{0ER}^{jki} &= -[\sin \theta_W Q_e N'_{j1} - \frac{Q_e \sin^2 \theta_W}{\cos \theta_W} N'_{j2} \\
&\quad + \frac{\sqrt{\cos 2\theta_W}}{\cos \theta_W} (T_e^3 - Q_e \sin^2 \theta_W) N'_{j3}] (\Gamma_{ER})_{ki}.
\end{aligned} \tag{72}$$

The one, two and three variable functions appearing in the decay $b \rightarrow sl^+l^-$ are [26]

$$F_1(x) = \frac{1}{12(x-1)^4}(x^3 - 6x^2 + 3x + 2 + 6x \log x), \quad (73)$$

$$F_2(x) = \frac{1}{12(x-1)^4}(2x^3 - 3x^2 - 6x + 1 - 6x^2 \log x), \quad (74)$$

$$F_3(x) = \frac{1}{2(x-1)^3}(x^2 - 4x + 3 + 2 \log x), \quad (75)$$

$$F_4(x) = \frac{1}{2(x-1)^3}(x^2 - 1 - 2x \log x), \quad (76)$$

$$F_5(x) = \frac{1}{36(x-1)^4}[7x^3 - 36x^2 + 45x - 16 + (18x - 12) \log x], \quad (77)$$

$$F_6(x) = \frac{1}{36(x-1)^4}(-11x^3 + 18x^2 - 9x + 2 + 6x^3 \log x), \quad (78)$$

$$F_7(x) = \frac{1}{12(x-1)^4}[x^3 + 10x^2 - 29x + 18 - (8x^2 - 6x - 8) \log x], \quad (79)$$

$$F_8(x) = \frac{1}{12(x-1)^4}[-7x^3 + 8x^2 + 11x - 12 - (2x^3 - 20x^2 + 24x) \log x], \quad (80)$$

$$F_9(x) = \frac{1}{2(x-1)^2}[x^2 - 7x + 6 + (3x + 2) \log x], \quad (81)$$

$$f(x) = -\frac{2}{3} - \frac{z}{x} + \begin{cases} 2 \left(1 + \frac{z}{2x}\right) \sqrt{\frac{z}{x} - 1} \tan^{-1} \left\{ \sqrt{\frac{z}{x} - 1} \right\}^{-1}, & \text{if } x < z \\ \left(1 + \frac{z}{2x}\right) \sqrt{1 - \frac{z}{x}} \left\{ \ln \frac{1 - \sqrt{1 - \frac{z}{x}}}{1 - \sqrt{1 - \frac{z}{x}}} - i\pi \right\}, & \text{if } x > z \end{cases} \quad (82)$$

$$F_0(x, y) = \frac{1}{x-y} \left[\frac{x}{x-1} \log x - (x \rightarrow y) \right], \quad (83)$$

$$G_0(x, y) = \frac{1}{x-y} \left[\frac{x^2}{x-1} \log x - \frac{3}{2}x - (x \rightarrow y) \right], \quad (84)$$

$$F(x, y) = -\frac{1}{x-y} \left[\frac{x}{(x-1)^2} \log x - \frac{1}{x-1} - (x \rightarrow y) \right], \quad (85)$$

$$G(x, y) = \frac{1}{x-y} \left[\frac{x^2}{(x-1)^2} \log x - \frac{1}{x-1} - (x \rightarrow y) \right], \quad (86)$$

$$G'(x, y, z) = \frac{1}{x-y} \left\{ \frac{1}{x-z} \left[\frac{x^2}{x-1} \log x - \frac{3}{2}x - (x \rightarrow z) \right] - (x \rightarrow y) \right\}, \quad (87)$$

$$F'(x, y, z) = -\frac{1}{x-y} \left\{ \frac{1}{x-z} \left[\frac{x}{x-1} \log x - (x \rightarrow z) \right] - (x \rightarrow y) \right\}. \quad (88)$$

References

- [1] M. Frank and S. Nie, to appear in Phys. Rev. **D65** (in press), hep-ph/0202154.
- [2] K. Abe *et al.*, BELLE Collaboration, hep-ex/0107072; Phys. Rev. Lett. **88**, 021801 (2002); Phys. Lett. **B511**, 151 (2001).
- [3] H. H. Asatrian, H. M. Asatrian, C. Greub and M. Walker, Phys. Lett. **B507**, 162 (2001); Phys. Rev. **D65**, 074004 (2002); C. Bobeth, M. Misiak and J. Urban, Nucl. Phys. **B574**, 291 (2000); A. Ali, E. Lunghi, C. Greub and G. Hiller, hep-ph/0112300.
- [4] B. Ginstein, M. J. Savage and M. B. Wise, Nucl. Phys. **B319**, 271 (1989); S. Bertolini, F. Borzumati, A. Masiero and G. Ridolfi, Nucl. Phys. **B353**, 591 (1991); A. Ali, G. F. Giudice and T. Mannel, Z. Phys. **C67**, 417 (1995); J. Hewett and J. D. Wells, Phys. Rev. **D55**, 5549 (1997); P. Cho, M. Misiak and D. Wyler, Phys. Rev. **D54**, 3329 (1996); T. Goto, Y. Okada, Y. Shimizu and M. Tanaka, Phys. Rev. **D55**, 4273 (1997); T. Goto, Y. Okada and Y. Shimizu, Phys. Rev. **D58**, 094006 (1998); Y. G. Kim, P. Ko and J. S. Lee, Nucl. Phys. **B544**, 64 (1999); E. Lunghi, A. Masiero, I. Scimemi and L. Silvestrini, Nucl. Phys. **B568**, 120 (2000).
- [5] E. Gabrielli and S. Khalil, Phys. Lett. **B530**, 133 (2002).
- [6] M. Gronau and S. Wakaizumi, Phys. Rev. Lett. **60**, 1814 (1992) .
- [7] M. Cvetč and J. Pati, Phys. Lett. **B135**, 57 (1984); R. N. Mohapatra and A. Rašin, Phys. Rev. **D54**, 5835 (1996); R. Kuchimanchi, Phys. Rev. Lett. **79**, 3486 (1996); R. N. Mohapatra, A. Rašin and G. Senjanović, Phys. Rev. Lett. **79**, 4744 (1997); C. S. Aulakh, K. Benakli, G. Senjanović, Phys. Rev. Lett. **79**, 2188 (1997); C. Aulakh, A. Melfo and G. Senjanović, Phys. Rev. **D57**, 4174 (1998).
- [8] R. Francis, M. Frank and C. S. Kalman, Phys. Rev. **D43**, 2369 (1991).

- [9] J. C. Pati and A. Salam, Phys. Rev. **D10**, 275 (1974); R. N. Mohapatra and J. C. Pati, Phys. Rev. **D11**, 566, 2558 (1975); G. Senjanović and R. N. Mohapatra, Phys. Rev. **D12**, 1502 (1975); R. N. Mohapatra and R. E. Marshak, Phys. Lett. **B91**, 222 (1980).
- [10] K. S. Babu and S.M. Barr, Phys. Rev. **D48**, 5354 (1993); **D50**, 3529 (1994); M. Frank, H. Hamidian and K. Puolamäki, Phys. Lett. **B456**, 179 (1999); Phys. Rev. **D60**, 095011 (1999); For a review and further references see e.g. R. N. Mohapatra, hep-ph/9801235.
- [11] G. Aldazabal, L. Ibanez and F. Quevedo, JHEP **0002**, 015 (2000); hep-ph/0005033.
- [12] Z. Chacko and R. N. Mohapatra, Phys. Rev. **D58**, 015003 (1998); B. Dutta and R. N. Mohapatra, Phys. Rev. **D59**, 015018 (1999).
- [13] R. Kuchimanchi and R. N. Mohapatra, Phys. Rev. **D48**, 4352 (1993).
- [14] K. Huitu and J. Maalampi, Phys. Lett. **B344**, 217 (1995); K. Huitu, J. Maalampi and M. Raidal, Phys. Lett. **B328**, 60 (1994); Nucl. Phys. **B420**, 449 (1994).
- [15] A. I. Vanshtein *et al.*, Yad. Fiz. **24**, 820 (1976)[Sov. J. Nucl. Phys. **24**, 427 (1976)]; N. G. Deshpande, J. Trampetic and K. Panrose, Phys. Rev. **D39**, 1461 (1989); C. S. Lim, T. Morozumi and A. I. Sanda, Phys. Lett. **B218**, 343 (1989); P. J. O'Donnell and H. K. Tung, Phys. Rev. **D43**, 2076 (1991).
- [16] M. Pospelov, Phys. Rev. **D56**, 259 (1997).
- [17] A. Heister *et al.*, ALEPH Collaboration, Phys. Lett. **B526**, 191 (2002).
- [18] G. C. Cho and K. Hagiwara, Phys. Lett. **B514**, 123 (2001).
- [19] M. Frank, H. Hamidian and K. Puolamäki, in [10].

- [20] L. J. Hall, V. A. Kostelecky and S. Raby, Nucl. Phys. **B267**, 415 (1986).
- [21] F. Borzumati, C. Greub, T. Hurth and D. Wyler, Phys. Rev. **D62**, 075005 (2000).
- [22] L. Everett, G. L. Kane, S. Rigolin, L.-T. Wang and T. T. Wang, JHEP **0201**, 022 (2002).
- [23] Particle Data Group, D. E. Groom *et al.*, Eur. Phys. J. **C15**, 1 (2000).
- [24] D. A. Demir, K. A. Olive and M. B. Voloshin, hep-ph/0204119.
- [25] E. Lunghi, A. Masiero, I. Scimeni and L. Silvestrini, in Ref. [4].
- [26] S. Bertolini, F. Borzumati, A. Masiero and G. Ridolfi, in Ref. [4].